THE IIOAB JOURNAL

VOLUME 9 : NO 5 : DECEMBER 2018 : ISSN 0976-3104

Institute of Integrative Omics and Applied Biotechnology Journal

Dear Esteemed Readers, Authors, and Colleagues,

I hope this letter finds you in good health and high spirits. It is my distinct pleasure to address you as the Editor-in-Chief of Integrative Omics and Applied Biotechnology (IIOAB) Journal, a multidisciplinary scientific journal that has always placed a profound emphasis on nurturing the involvement of young scientists and championing the significance of an interdisciplinary approach.

At Integrative Omics and Applied Biotechnology (IIOAB) Journal, we firmly believe in the transformative power of science and innovation, and we recognize that it is the vigor and enthusiasm of young minds that often drive the most groundbreaking discoveries. We actively encourage students, early-career researchers, and scientists to submit their work and engage in meaningful discourse within the pages of our journal. We take pride in providing a platform for these emerging researchers to share their novel ideas and findings with the broader scientific community.

In today's rapidly evolving scientific landscape, it is increasingly evident that the challenges we face require a collaborative and interdisciplinary approach. The most complex problems demand a diverse set of perspectives and expertise. Integrative Omics and Applied Biotechnology (IIOAB) Journal has consistently promoted and celebrated this multidisciplinary ethos. We believe that by crossing traditional disciplinary boundaries, we can unlock new avenues for discovery, innovation, and progress. This philosophy has been at the heart of our journal's mission, and we remain dedicated to publishing research that exemplifies the power of interdisciplinary collaboration.

Our journal continues to serve as a hub for knowledge exchange, providing a platform for researchers from various fields to come together and share their insights, experiences, and research outcomes. The collaborative spirit within our community is truly inspiring, and I am immensely proud of the role that IIOAB journal plays in fostering such partnerships.

As we move forward, I encourage each and every one of you to continue supporting our mission. Whether you are a seasoned researcher, a young scientist embarking on your career, or a reader with a thirst for knowledge, your involvement in our journal is invaluable. By working together and embracing interdisciplinary perspectives, we can address the most pressing challenges facing humanity, from climate change and public health to technological advancements and social issues.

I would like to extend my gratitude to our authors, reviewers, editorial board members, and readers for their unwavering support. Your dedication is what makes IIOAB Journal the thriving scientific community it is today. Together, we will continue to explore the frontiers of knowledge and pioneer new approaches to solving the world's most complex problems.

Thank you for being a part of our journey, and for your commitment to advancing science through the pages of IIOAB Journal.

Yours sincerely,

Vasco Azevedo

Vasco Azevedo, Editor-in-Chief
Integrative Omics and Applied Biotechnology
(IIOAB) Journal

Prof. Vasco Azevedo
Federal University of Minas Gerais
Brazil

Editor-in-Chief

Integrative Omics and Applied Biotechnology (IIOAB) Journal Editorial Board:

REVIEW

A REVIEW ON THE MECHANICAL PROPERTIES AND ENVIRONMENTAL IMPACT OF HOLLOW GLASS MICROSPHERE EPOXY COMPOSITES

Sunny Bhatia*, Moin Khan, Himanshu Sengar, Vivek Bhatia

Department of Automobile Engineering, Manav Rachna International Institute of Research and Studies, Faridabad, INDIA

ISSN 0976-3104

ABSTRACT

The use of hollow glass microspheres (HGM) in composites is creating new opportunities in the composites industry. HGM consists of stiff glass hollow sphere filled with inert gas resulting in some specific properties like low weight, reduced dielectric constant, and reduced thermal conductivity. The typical wall thickness of HGMs is lying in between 0.5-2.0 µm and diameter 10-200 µm. On the basis of these properties, HGMs have been employed in the manufacturing of various composites for diverse applications. Therefore, the need of light-weight and high-strength materials for modern engineering applications may fulfill by the HGM composites. HGMs not only amending the properties but also ensuring the stability of molded articles by reducing viscosity and shrinkage of the composites. In this work, a comprehensive review on the properties of hollow glass microsphere (HGM) reinforced epoxy composites is presented. The summary of the paper shows the appropriateness of HGM-epoxy composites as an encouraging material for aerospace, automotive and cryogenic applications. The main focus area of the present study is the mechanical and environmental performance of the HGM composites.

KEY WORDS
Hollow glass microspheres, composite, epoxy, environment, mechanical properties

Received: 19 April 2018
Accepted: 26 May 2018
Published: 1 Oct 2018

***Corresponding Author**
Email:
sunny576bhatia@gmail.com
Tel.: +91-8826004666

INTRODUCTION

Composites are the materials produced employing two or more materials with different properties which on joining having assorted properties of both the constituents. The composite materials possess the indispensable properties borrowed from the best features of the two joined constituents. This material has the high strength to weight ratio and firm, fragile and other privative attributes of one material are concealed by the other one. In recent times, polymer composites are rapidly substituting the standard materials in various designing and product development in the engineering sector. Traditional materials and their modifications have a limited set of properties with a minor chance of improvements. On the other hand, composite materials can provide better quality control and required assortment of characteristics as per the application requirement. A proper blend of materials properties like specific modulus, a certain quality, low thickness etc. is doable in composites. The applications of composite materials are not limited to some particular areas. It also marked its presence in the space industry besides other common engineering industries owing to its sturdiness and potentials [1,2]. A thin walled sphere filled with inert gas or vacuum inside and a hard glass at the periphery are termed as hollow glass microspheres (HGMs). It is also named as hollow glass bead or glass bubbles or microballoons [3,4]. Syntactic foam is an example of HGM filled polymer composites [5]. The hollow glass microspheres have properties like feathery light, high specific area, inexpensive, low dielectric constant, flexible and noncorrosive. Additionally, the fragile microbeads are chemically strong, inflammable, unyielded and have excellent water resistance. The microspheres can be used in coatings, putty, artificial stones, emulsion explosives etc. [6–10]. It can also be used in oil and gas extraction industries as drilling fluid owing to its low density. It is also used to make superior optical glasses for visual resonators. Presently, the HGM reinforced composites especially syntactic foam are used to fabricate the gadgets employed for marine applications, deep sea exploration, ship bodies, helicopter and jet engine parts, detector instruments, noise reduction materials, sports merchandises. In the recent time, there is an increasing demand for the materials with low density and a high Young's modulus for various engineering applications. Therefore, HGM reinforced ploymer composites are gaining attention day by day. Foam glass owed Young's modulus and density of typically 1 GPa and 130 kgm^{-3}, respectively [11,12]. Moreover, it could be blown up to a full-size bubble of 2 mm diameter and frequently used to prepare HGM composite [12]. In the present article, the major focus of the study is the mechanical properties of the HGM reinforced composites reported in the various literatures. Additionally, the environmental and economic aspects of the same are also addressed in the article.

MECHANICAL PROPERTIES OF HGM COMPOSITES

In this paper, the mechanical properties of rarely reconnoitered HGM reinforced polymer composites are summarized. In the recent years, the structural properties of syntactic foams are studied by several researchers.

Compressive strength

The compressive strength of HGMs filled epoxy composites are decreased with increasing volume fractions of the reinforcements [Fig. 1]. Additionally, higher density HGMs stimulates higher compressive strength of the composites. It can be marked from the plots [Fig. 1] that a stress plateau/valley exists in the plastic deformation region. The valley indicated the presence of broken HGMs owing to the compressive loading.

IIOAB JOURNAL
ISSN: 0976-3104

The existence of stress plateau represents the high-energy absorbing capability of the composites. The main fracture mechanism of this type of composite is crushing and crumbling of HGMs.

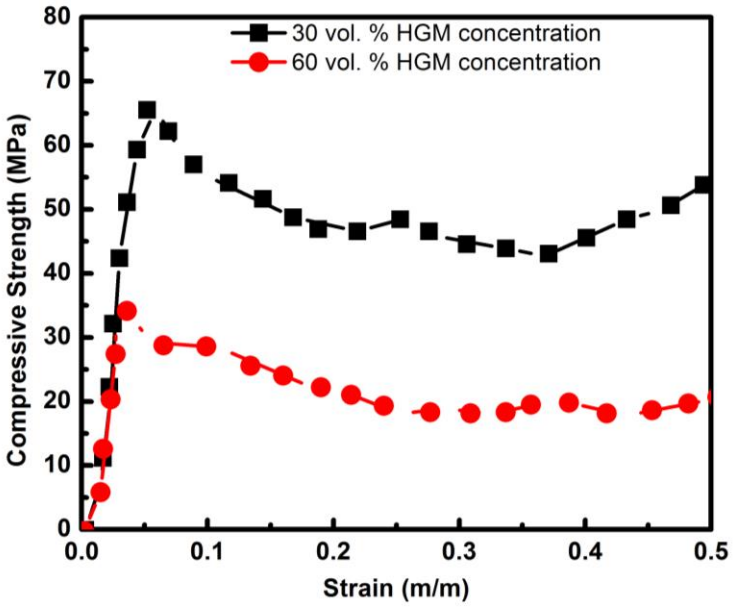

Fig. 1: Compressive stress-strain curve of epoxy matrix containing HGMs of 220 kg/m^3 in 60 and 30 vol% (Reconstructed from reference [13]).

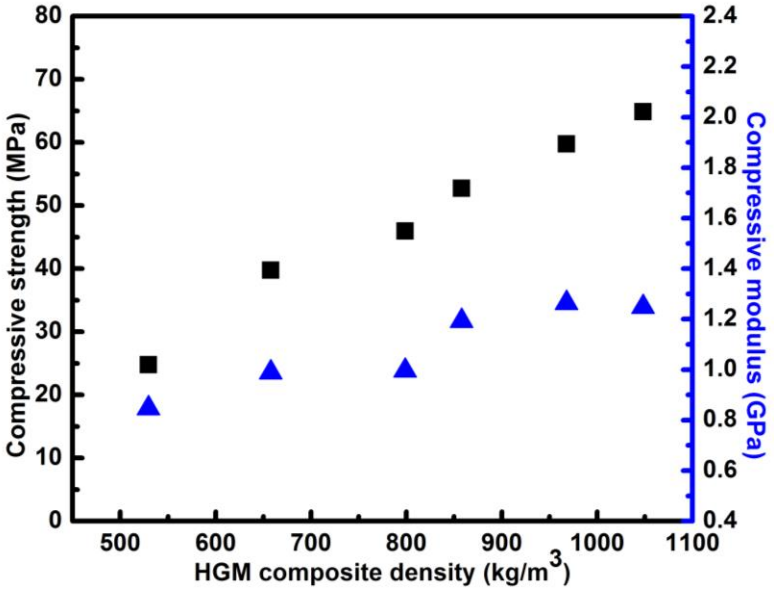

Fig. 2: Variation in compressive strength and modulus regarding the HGM composite density (Reconstructed from reference [13]).

The compressive strength/modulus versus density plots of HGM filled composites are recreated from [13] and shown in [Fig. 2]. This Figure is showing an increase in compressive strength with increasing density of reinforcements in composites. Other researchers have also reported the similar general trend [14–17]. Conversely, there is an insignificant change in compressive strength by changing the wall thickness and volume fraction of HGMs. Some papers depicted that broken HGM particles acted as solid fillers in the resin and improved the density of the composites. There is no specific trend reported in compressive modulus concerning density, and it was strongly dependent on the wall thickness of fillers. Thick walled HGMs increased the modulus whereas, thin-walled decreased the same [18]. [Table 1] depicts the maximum compressive strength of the various types of HGM polymer composites. When the HGM concentrations in the composites were less than or equal to 10%, the maximum compressive strength was reported. Higher HGM concentration might assist in improving Young's modulus in some composites. In

ISSN: 0976-3104

some cases, it was observed that the addition of HGMs in polymer have no significant improvement in compressive strength or Young's modulus.

Table 1: The maximum compressive strengths of HGM based composites reported in literature

Matrix	Type and quantity of HGM	Young's modulus (MPa)	Compressive strength (MPa)	Ref.
Borosilicate glass	K46 (10%)	1388	19.0	[19]
Borosilicate glass	S60HS (10%)	1613	23.5	
Borosilicate glass	iM16K (10%)	1535	22.7	
Borosilicate glass	iM30K (10%)	1655	25.0	
Borosilicate glass	(383HS) FAC (10%)	1103	9.8	[20]
Araldite GY257	-	1648	104	[16]
Araldite GY257	K15 (10%)	1472	90.6	
Araldite GY257	S22 (10%)	1258	67.4	
Araldite GY257	S22 (20%)	1287	61.8	
Araldite GY257	K46 (10%)	1660	98.7	

Tensile strength

[Fig. 3] exhibits a representative stress-strain curve of HGM reinforced polymer composites under tensile loading. The plots were reconstructed from the data reported in reference [21]. The chosen composites contained 30 and 60 vol% HGMs of density 220 kg/m^3. The composites exhibited brittle type failure under tensile loading. Therefore, reduced tensile properties restricted the use of composite to the applications where loading conditions are the compressive type. It was reported that the strength might increase to some extent when HGMs-epoxy interfacial bonding is strong enough. The firm interfacial bonding assists in proper load sharing among the constituents. It can be examined from the [Fig. 4] that the tensile modulus of HGM composites improved with the incorporation of thick-walled HGMs. The high compressive strength of HGM composites is due to proper load distribution along with cracks closure ability during loaded conditions [22,23]. On the contrary, tensile load assisted in opening up the interfacial cracks resulted in poor strength. The tensile strength of the HGM composites is mainly dependent on polymer strength as well as fabrication defects. This problem might be solved by further reinforcing the HGM composites with glass fibers, carbon fibers, carbon nanotubes etc. [18, 24]. [Table 2] exhibits the maximum tensile strengths of HGM composites reported in the literature. It can be inferred from the table that low HGM concentration in the composites leads to better tensile strength. Apart from that untreated or medium size HGMs are exhibiting better strength than the other one. The yield strength of the composites did not follow any trend. In some cases, it was increased with the increment in HGM concentrations. On the other hand, the reverse is also true for some other instances.

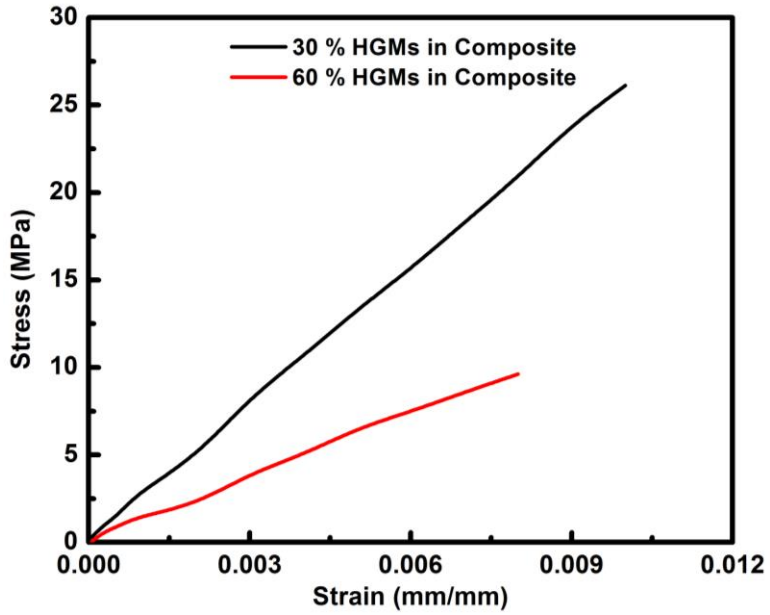

Fig. 3: Tensile stress-strain curves of HGM composites containing HGMs of 220 kg/m^3 density (Reconstructed from Reference [21]).

IIOAB JOURNAL
ISSN: 0976-3104

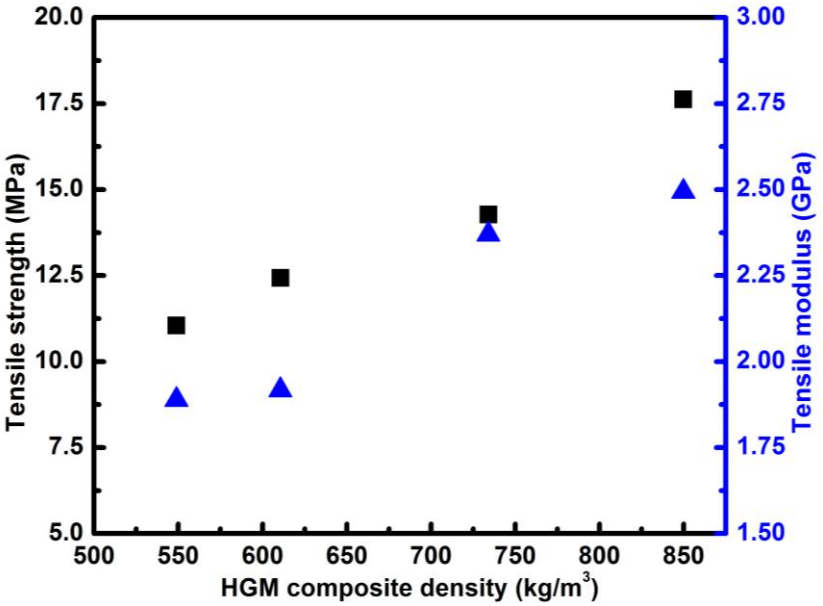

Fig. 4: Variation in tensile strength and modulus regarding the HGM composite density (Reconstructed from reference [21]).

Table 2: The maximum tensile strengths of various HGM based composites reported in literature

Matrix	Type and quantity of HGM	Young's modulus (MPa)	Tensile strength (MPa)	Ref.
Poly butylene succinate	-	330	34.7	[25]
Poly butylene succinate	T60 (05%)	355	32.2	
Poly butylene succinate	T60 (10%)	371	25.3	
Poly butylene succinate	T60 (15%)	439	23.7	
Poly butylene succinate	T60 (20%)	464	18.1	
Acrylonitrile Butadiene Styrene (ABS)	-	41	29.6	[26]
Acrylonitrile Butadiene Styrene (ABS)	TK70 (05%)	42	30.2	
Acrylonitrile Butadiene Styrene (ABS)	TK70 (10%)	41	30.7	
Acrylonitrile Butadiene Styrene (ABS)	TK70 (15%)	40	32.2	
Acrylonitrile Butadiene Styrene (ABS)	TK70 (20%)	38	32.3	
Polypropylene	-	33	29.3	[27]
Polypropylene	A-Glass 3000 (05%)	30	25.5	
Polypropylene	A-Glass 3000U (05%)	29	23.7	
Poly Vinyl Chloride (PVC)	-	48	33.8	[28]
Poly Vinyl Chloride (PVC)	HGMs-15µm (05%)	47	42.0	
Poly Vinyl Chloride (PVC)	HGMm-24µm (05%)	49	38.4	
Poly Vinyl Chloride (PVC)	HGMb-96µm (05%)	48	36.9	

Flexural properties

In flexural load-displacement curves, the load varies linearly with respect to displacement until failure occurs [29]. The flexural behavior of HGM filled composites were primarily determined by the tensile properties of the composites. The graphs of flexural strength/modulus versus density for thin and thick-walled HGMs were recreated from reference [15] and exhibited in [Fig. 5] and [Fig. 6]. The lower values of flexural strength and premature failure of HGM containing composites were articulated by the existence of matrix porosity and surface defects. Additionally, it was observed that the flexural modulus was slightly increased with increasing volume fraction of thin-walled HGMs. Conversely, incorporation of the higher amount of thick-walled HGMs reduced the flexural modulus of the composites significantly as shown in [Fig. 6]. Therefore it can be expounded that the surface roughness and air voids in the matrix hampered the flexural strength of the composites in a great extent and leads to premature failure in the HGM filled composites [18].

From [Table 3], it can be reiterated that in some instances when low-density HGM was present in relatively higher amount exhibited high flexural modulus and strength than its counterparts. Also, the improvement reported in the flexural strength is marginal in some composites, and there is deterioration in flexural strength than the matrix in some other composites. Therefore, the addition of HGMs imposed positive changes regarding mechanical properties in selective epoxies only.

IIOAB JOURNAL
ISSN: 0976-3104

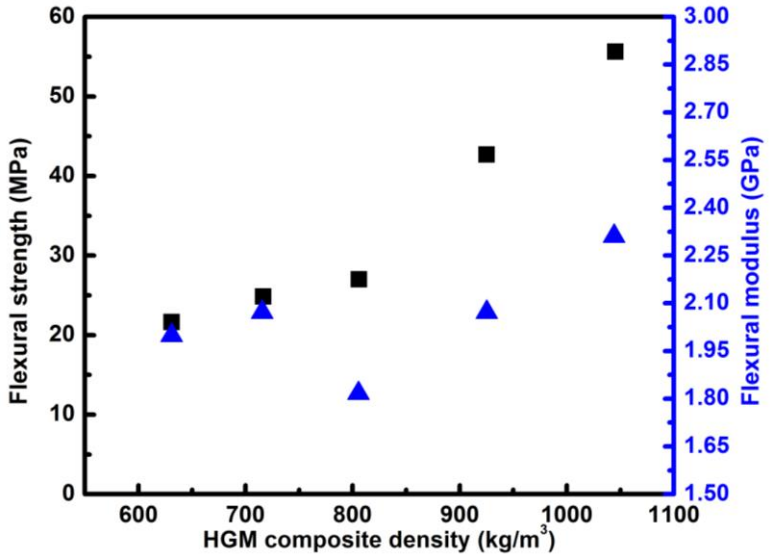

Fig. 5: Variation in flexural strength and modulus regarding the HGM composite density containing HGMs of 150 kg/m^3 density (Reconstructed from Reference [15]).

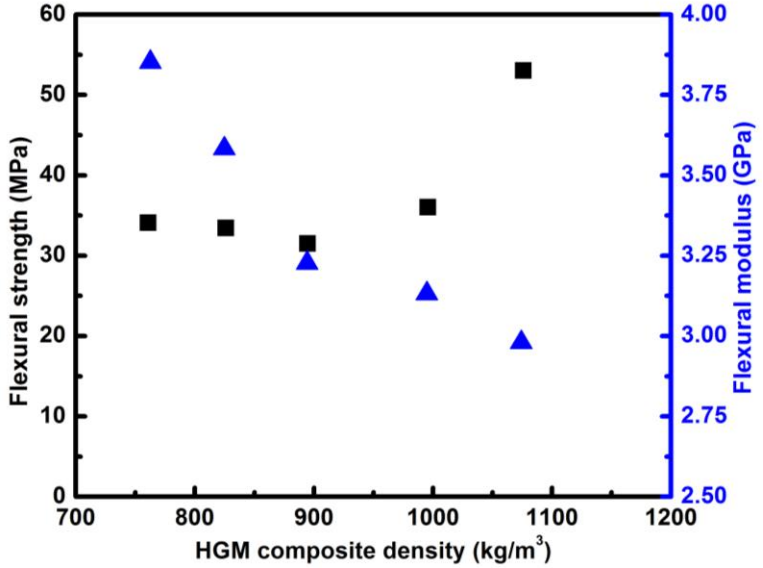

Fig. 6: Variation in flexural strength and modulus regarding the HGM composite density containing HGMs of 460 kg/m^3 density (Reconstructed from Reference [15]).

Table 3: The maximum flexural strengths of various HGM based composites reported in literature

Matrix	Type and quantity of HGM	Flexural modulus (MPa)	Flexural Strength	Ref.
Vinyl ester	-	3229	103.5	[30]
Vinyl ester	HGM220 (50%)	3523	58.0	
Vinyl ester	HGM220 (60%)	3634	54.1	
Vinyl ester	HGM320 (30%)	2864	46.2	
Vinyl ester	HGM320 (60%)	3571	34.3	
Vinyl ester	HGM460 (30%)	2371	24.4	
Vinyl ester	HGM460 (60%)	3753	25.2	
Acrylonitrile Butadiene Styrene (ABS)	-	41	35.5	[26]
Acrylonitrile Butadiene Styrene (ABS)	TK70 (05%)	42	36.9	
Acrylonitrile Butadiene Styrene (ABS)	TK70 (20%)	38	39.0	

BRIEF OVERVIEW ON MECHANICAL PROPERTIES OF HGM COMPOSITES

Fu et al. [31] reiterated that the particle size, bonding capability and load are the deciding factors for stiffness, strength and toughness in particulate composites. Stiffness basically depends on load bearing capability of reinforcement rather than bonding whereas, toughness depends on bonding strength. Kinloch et al. [32] found that the mechanical and physical properties of thermosets or thermoplastic resins were

IIOAB JOURNAL
ISSN: 0976-3104

significantly improved using HGMs as reinforcement. As per the investigation of Sahu and Broutman [33] the material with low melting viscosity or isotropy can be produced by associating glass beads into polyester and epoxy resins. They studied the mechanical behaviour along with fracture analysis of the same too. Mallick and Broutman [34] investigated the strength and fracture behavior of HGM filled epoxy composites. They did not observed better strength in HGM composite since critical crack size is not affected by the interparticle distance. Swetha and Kumar [16] prepared HGM composites of various densities using stir casting process and studied their mechanical properties. They found that the strength of the composite is high when the density of the HGM is high in the composite. Additionally, energy absorption capacity of the composite is increased till the addition of 40% HGM. The mechanical properties of HGM composites consisting HGMs of different diameter are investigated by d'Almeida [35]. He represented rupture of the microspheres as a single damage parameter. This investigation concluded that the ratio of wall thickness and mean diameter of the microspheres is the useful fabrication parameter. Yung et al. [36] studied the dielectric properties of HGM (0-51.3 vol.%) filled epoxy composites. They observed that the dielectric constant and dielectric losses decreased with increased HGM content. Apart from that the coefficient of thermal expansion (CTE) and the glass transition temperature (Tg) of the composites are enhanced significantly. Similar results were also observed by Park et al. [37] in HGM (0-2 wt.%) filled diglycidyl ether of bisphenol A (DGEBA) composites. They also found that the mechanical and interfacial properties of the HGM filled DGEBA are considerably higher than the neat DGEBA. Kim and Khamis [38] studied the fracture and impact behaviours of HGM (0-0.65 vol.%) filled epoxy resin composites. The addition slightly reduced the impact force and marginally increased the specific flexural modulus at the expense of specific fracture toughness and specific flexural strength. Hu et al. [39] studied the influence of broken HGMs on density, mechanical property and thermal conductivity in HGM filled silicon rubber composites. They found that these properties are enhanced even after the HGMs are broken inside the composites. Li et al. [25] investigated the morphology, melting/crystallization behavior, mechanical properties and thermal stability of HGM filled poly(butylene succinate) (PBS) composites. They observed that the crystallization rate and thermal stability of the composites were increased without hampering the crystalline nature. Additionally, the storage modulus of the composite is increased too. Huang and Li [40] developed a model for randomly distributed glass microspheres in epoxy using finite element modelling (FEM). They studied the elastic behavior and failure mechanism of different volume fractions of HGM filled composites. In this investigation they found that adjoining of adjacent microcracks along with voids due to broken HGMs are forming macro-cracks and propagating in a particular direction in the composite. Wang et al. [41] fabricated HGM-bisphenol A dicyanate ester (BADCy) composite using mechanical mixing followed by a stepped curing process. They found improved mechanical properties such as impact strength, flexural strength, flexural modulus and storage modulus without compromising its thermal properties. Im et al. [42] found that the HGM filled thermoplastic polyurethane composite have superior mechanical properties and a lesser amount of water adsorption properties for sonar encapsulating materials. Li et al. [43] studied the strain rates sensitivity of HGM containing epoxy syntactic foams in finite element stress analysis. As per the study, failures occurred in the composite due to crushing of glass microspheres and shear cracking of the epoxy matrix. Higher strain rate leads to the higher microsphere cracking and higher matrix debonding. Liang [26] studied the tensile and flexural properties of HGM filled ABS copolymer at room temperature. Increase in Young's modulus was observed till 5% volume fraction of HGMs. Till 15 vol.% HGM, ultimate tensile strength increased and remain constant afterwards. The tensile and impact strength of the HGM filled PVC composites were investigated by Liang [28]. He reported slightly lower yield strength with increasing HGM volume fraction in the PVC. On the other hand, somewhat better UTS of the composites was observed when volume fraction of HGMs lying in between 0–20%. Ferreira et al. [44] studied the mechanical behavior of hybrid composites prepared by HGMs and short fibre reinforcements. In terms of specific values, both flexural and compressive stiffness and impact absorbed energy increase with microsphere content.

ENVIRONMENTAL IMPACT OF HGM COMPOSITES

The composites fabricated using natural fibers are attracting attention among scientific and industrial communities owing to growing environmental concerns and more stringent norms [45]. These composites have several advantages over synthetic fiber composites such as low abrasion in processing, lower environmental impact, low cost, excellent specific properties and reasonable mechanical properties [46,47]. These fibers are generally employed in thermosets (e.g. polyester etc.) and thermoplastics (e.g. polypropylene, polyethylene etc.) composites. Among several thermoplastic polymers, Polypropylene (PP) is one of the commonly used semicrystalline thermoplastic. It has a set of attractive properties like high melting/service temperature, good chemical strength, higher stiffness, excellent durability, lightweight, easy to process and cost-effective [48,49]. The applications of neat PP are limited despite having many attractive properties [50]. The drawbacks might be subdued if vegetal, inorganic or mineral reinforcements are employed in PP. Likewise, other plastics whether it is thermoset or thermoplastic possess excellent properties but barely used in the unadulterated form for any structural applications. The reinforcement is always required to make it suitable for such type of applications. The composite development revolves around the natural or recyclable fillers are always encouraged for the betterment of human civilization. Hollow glass microspheres (HGM) are inorganic and spherical mineral fillers [39]. They are finely dispersed, free-flowing thin-walled powder particles with good thermal properties and low density [4]. As discussed in the previous section, the mechanical properties especially compressive strength of HGM containing composites are comparatively better than the neat epoxies in some instances. Additionally, HGMs are inorganic, recyclable and did not harm the environment. Therefore, HGM containing composites

IIOAB JOURNAL
ISSN: 0976-3104

are considered as environmental friendly material, and regular attempts are going on for improving its properties worldwide.

CONCLUSION

HGM composites are having lower densities than the neat epoxies owing to the presence of hollow glass microbeads. The density of the composite will further go down if the thin-walled microbeads concentration is increased in it. The concentration of the filler contents is the deciding factors for the various properties of the composites, especially the mechanical one. The inferences drawn from the review indicates that lower concentration of the microspheres in most of the epoxy composites exhibited improved compressive strength, unlike yield strength. A similar trend was also reported for the tensile strength of HGM composites. However, the values of yield strength are more or less scattered and not following any specific pattern. It has a strong dependency on the epoxies as well as types of HGMs used. A relatively higher HGM concentration in the composites exhibited better flexural strength and modulus than its counterparts. But the improvement in the flexural strength is insignificant. In some instances, the mechanical properties are even weaker than the virgin matrix. Therefore, the choice of polymer and type of HGM should be as per the focused application area. The glass beads could be prepared from waste materials or as a byproduct of some critical industrial processes along with very high recyclability potential. Therefore, the use of glass microbead composite material is not imposing any potential harm to the ecosystem. It could be considered as a green material as per grown environmental concerns. It has a potential to replace many metals or composites in various industries. For this, extensive research efforts in multiple aspects are needed to scale the gap between HGM composites and conventional materials.

CONFLICT OF INTEREST
There is no conflict of interest

ACKNOWLEDGEMENTS
Authors wish to thank Dr. Anil from Accendere Knowledge Management Services, CL Educate, New Delhi for his contribution in manuscript preparation

FINANCIAL DISCLOSURE
None

REFERENCES

[1] Hull D, Clyne TW. [1996] An introduction to composite materials (Cambridge university press).
[2] Hahn HT, Tsai SW. [1980] Introduction to composite materials (CRC Press).
[3] Mutua FN, Lin P, Koech JK, Wang Y. [2012] Surface Modification of Hollow Glass Microspheres.
[4] Budov VV. [1994] Hollow glass microspheres. use, properties, and technology. Glass Ceram. 51: 230–235.
[5] Landrock AH. [1995] Handbook of plastic foams: types, properties, manufacture and applications (Elsevier).
[6] Yu X, Shen Z, Xu Z, Wang S. [2007] Fabrication and structural characterization of metal films coated on cenosphere particles by magnetron sputtering deposition, Appl Surf Sci. 253: 7082–7088.
[7] Anshits AG, Anshits NN, Deribas AA, et al. [2005] Detonation Velocity of Emulsion Explosives Containing Cenospheres, Combust Explos Shock Waves. 41: 591–598.
[8] Medvedev AE, Fomin VM, Reshetnyak AY. [2008] Mechanism of detonation of emulsion explosives with microballoons. Shock Waves. 18(2): 107-115.
[9] Butler WB, Mearing MA. [1985] Fly Ash Beneficiation and Utilization in Theory and in Practice, MRS Online Proc Libr Arch. 65: 11-17.
[10] Shukla S, Seal S, Akesson J, Oder R, Carter R, Rahman Z. [2001] Study of mechanism of electroless copper coating of fly-ash cenosphere particles. Appl Surf Sci. 181: 35–50.
[11] Morgan JS, Wood JL, Bradt RC. [1981] Cell size effects on the strength of foamed glass, Mater Sci Eng. 47:37–42.
[12] Verweij H, Veeneman D. [1985] Hollow glass microsphere composites: preparation and properties, J Mater Sci. 20: 1069–1078.
[13] Gupta N, Woldesenbet E, Sankaran S. [2001] Studies on compressive failure features in syntactic foam material, J Mater Sci 36: 4485–4491.
[14] Gupta N, Woldesenbet E, Mensah P. [2004] Compression properties of syntactic foams: effect of cenosphere radius ratio and specimen aspect ratio, Compos Part Appl Sci Manuf. 35: 103–111.
[15] Wouterson EM, Boey FY, Hu X, Wong SC. [2005] Specific properties and fracture toughness of syntactic foam: Effect of foam microstructures, Compos Sci Technol. 65: 1840–1850.
[16] Swetha C, Kumar R. [2011] Quasi-static uni-axial compression behaviour of hollow glass microspheres/epoxy based syntactic foams, Mater Des. 32: 4152–4163.
[17] Kim HS, Plubrai P. [2004] Manufacturing and failure mechanisms of syntactic foam under compression, Compos Part Appl Sci Manuf. 35: 1009–1015.
[18] Pinisetty D, Shunmugasamy VC, Gupta N. [2015] Hollow glass microspheres in thermosets—epoxy syntactic foams. Hollow Glass Microspheres for Plastics, Elastomers, and Adhesives Compounds (Elsevier) pp 147–174.
[19] Ren S, Li X, Zhang X, et al. [2017] Mechanical properties and high-temperature resistance of the hollow glass microspheres/borosilicate glass composite with different particle size, J Alloys Comp. 722: 321–329.
[20] Ren S, Tao X, Ma X, et al. [2018] Fabrication of fly ash cenospheres-hollow glass microspheres, borosilicate glass composites for high temperature application, Ceram Int. 44: 1147–1155.
[21] Gupta N, Nagorny R. [2006] Tensile properties of glass microballoon-epoxy resin syntactic foams. J Appl Polym Sci. 102: 1254–1261.
[22] Tagliavia G, Porfiri M, Gupta N. [2010] Analysis of hollow inclusion–matrix debonding in particulate composites, Int J Solids Struct. 47: 2164–2177.
[23] Tagliavia G, Porfiri M, Gupta N. [2011] Elastic interaction of interfacial spherical-cap cracks in hollow particle filled composites. Int J Solids Struct. 48: 1141–1153.
[24] Gupta N, Pinisetty D, Shunmugasamy VC. [2013] Reinforced polymer matrix syntactic foams: effect of nano and micro-scale reinforcement (Springer Science & Business Media).
[25] Li J, Luo X, Lin X. [2013] Preparation and characterization of hollow glass microsphere reinforced poly (butylene succinate) composites, Mater Des. 46: 902–909.

[26] Liang JZ. [2005] Tensile and flexural properties of hollow glass bead-filled ABS composites, J Elastomers Plast. 37: 361–370.
[27] Liang JZ, Li RKY. [2000] Effect of filler content and surface treatment on the tensile properties of glass-bead-filled polypropylene composites, Polym Int. 49: 170–174.
[28] Liang JZ. [2002] Tensile and Impact Properties of Hollow Glass Bead-Filled PVC Composites, Macromol Mater Eng. 287: 588–591.
[29] Maharsia R, Gupta N, Jerro HD. [2006] Investigation of flexural strength properties of rubber and nanoclay reinforced hybrid syntactic foams, Mater Sci Eng. A 417: 249–258.
[30] Tagliavia G, Porfiri M, Gupta N. [2010] Analysis of flexural properties of hollow-particle filled composites. Compos Part B Eng. 41: 86–93.
[31] Fu SY, Feng XQ, Lauke B, Mai YW. [2008] Effects of particle size, particle/matrix interface adhesion and particle loading on mechanical properties of particulate–polymer composites Compos Part B Eng. 39: 933–961.
[32] Kinloch AJ. [2013] Fracture behaviour of polymers (Springer Science & Business Media).
[33] Sahu S, Broutman LJ. [1972] Mechanical properties of particulate composites, Polym Eng Sci. 12: 91–100
[34] Mallick PK, Broutman LJ. [1975] Mechanical and fracture behaviour of glass bead filled epoxy composites, Mater Sci Eng. 18: 63–73.
[35] d'Almeida JRM. [1999] An analysis of the effect of the diameters of glass microspheres on the mechanical behavior of glass-microsphere/epoxy-matrix composites, Compos Sci Technol. 59: 2087–2091.
[36] Yung KC, Zhu BL, Yue TM, Xie CS. [2009] Preparation and properties of hollow glass microsphere-filled epoxy-matrix composites, Compos Sci Technol. 69: 260–264.
[37] Park SJ, Jin FL, Lee C. [2005] Preparation and physical properties of hollow glass microspheres-reinforced epoxy matrix resins. Mater, Sci Eng A 402: 335–340.
[38] Kim HS, Khamis MA. [2001] Fracture and impact behaviours of hollow micro-sphere/epoxy resin composites, Compos Part Appl Sci Manuf. 32: 1311–1317.
[39] Hu Y, Mei R, An Z, Zhang J. [2013] Silicon rubber/hollow glass microsphere composites: Influence of broken hollow glass microsphere on mechanical and thermal insulation property, Compos Sci Technol. 79: 64–69.
[40] Huang R, Li P. [2015] Elastic behaviour and failure mechanism in epoxy syntactic foams: The effect of glass microballoon volume fractions, Compos Part B Eng. 78: 401–408.
[41] Wang J, Liang G, He S, Yang L. [2010] Curing behavior and mechanical properties of hollow glass microsphere/bisphenol a dicyanate ester composites, J Appl Polym Sci. 118: 1252–1256.
[42] Im H, Roh SC, Kim CK. [2011] Fabrication of novel polyurethane elastomer composites containing hollow glass microspheres and their underwater applications, Ind Eng Chem Res. 50: 7305–7312.
[43] Li P, Petrinic N, Siviour CR, Froud R, Reed JM. [2009] Strain rate dependent compressive properties of glass microballoon epoxy syntactic foams, Mater Sci Eng A. 515: 19–25.
[44] Ferreira JA M, Capela C, Costa JD. [2010] A study of the mechanical behaviour on fibre reinforced hollow microspheres hybrid composites, Compos Part Appl Sci Manuf. 41: 345–352.
[45] Saha P, Chowdhury S, Roy D, et al. [2016] A brief review on the chemical modifications of lignocellulosic fibers for durable engineering composites, Polym Bull. 73: 587–620.
[46] Almeida Jr JHS, Amico SC, Botelho EC, Amado FDR. [2013] Hybridization effect on the mechanical properties of curaua/glass fiber composites, Compos Part B Eng. 55: 492–497.
[47] Karaduman Y, Onal L, Rawal A. [2015] Effect of stacking sequence on mechanical properties of hybrid flax/jute fibers reinforced thermoplastic composites, Polym Compos. 36: 2167–2173.
[48] Pigatto C, Santos Almeida JH, Luiz Ornaghi H, Rodríguez AL, Mählmann CM, Amico SC. [2012] Study of polypropylene/ethylene-propylene-diene monomer blends reinforced with sisal fibers, Polym Compos. 33: 2262–2270.
[49] Doumbia AS, Castro M, Jouannet D, et al. [2015] Flax/polypropylene composites for lightened structures: Multiscale analysis of process and fibre parameters, Mater Des 87: 331–341.
[50] Pedrazzoli D, Pegoretti A. [2014] Long-term creep behavior of polypropylene/fumed silica nanocomposites estimated by time–temperature and time–strain superposition approaches, Polym Bull. 71: 2247–2268.

IIOAB JOURNAL

ARTICLE

SIGNIFICANCE OF USING THE MANDIBULAR CANINE INDEX IN GENDER DETERMINATION

Christy Jacob*, Elham Izadpanahian, Madhura Jadhav, Amol Patil

Dept. of Orthodontics and Dentofacial Orthopedics, Bharati Vidyapeeth (Deemed to be University) Dental College and Hospital, Pune, Maharashtra, INDIA

ISSN 0976-3104

ABSTRACT

A study was conducted using the mandibular canine index to evaluate its significance in gender determination. 1000 casts were measured and the index calculated in the Maharashtrian population aged 18-25 years. The study showed to have 40.6% accuracy in males and 70.2% accuracy in females. Therefore proving that MCI can be used as a supplemental tool in forensic odontology and should not be relied on solely for gender determination.

KEY WORDS
Mandibular Canine, Index, Forensic Odontology, Mandibular Canine Index, MCI

INTRODUCTION

Forensic dentistry is an important field in dentistry, especially in aiding post mortem reports to determine cause of death by studying the bite marks etc. Along with it, forensic odontology can also be used in gender determination using cranium remains. This study is done to see the usefulness of using the mandibular canine index to find the gender of the individual.

Enamel being the hardest substance of the human body make teeth a very invaluable material to be used for genetic, forensic and other purposes. Especially in the case of forensic odontology when the body has undergone decomposition, the enamel being the most durable and stable tissue in the body will present as a key to investigation [1, 2].

Canines are considered to be the longest permanent teeth in the mouth. They are also called 'corner stone' in the dentition. The mean age of eruption of mandibular canines is 10.87 years [3]. Canines are used in forensic studies due to (i) its durability in the mouth, (ii) they are the last teeth to be extracted with respect to age (iii)it is the tooth which is least affected by calculus or caries, thus won't be subject to gross deformity or periodontal diseases (iv)They are very durable to various natural calamities [4].

Although DNA tests provide the most accurate information in regard to gender identification, the purpose of this study is to check the reliability using the mandibular canine index to determine the gender and to provide additional information on the sex identification.

Received: 11 July 2018
Accepted: 30 July 2018
Published: 10 Oct 2018

MATERIALS AND METHODS

One thousand mandibular casts were recorded for this study, out of which five hundred casts were of females and five hundred of male individuals from a majority of Maharashtrian population, within the age group of 18-25 years. Patients were informed about using their casts for study purposes and written consent was taken. Ethical approval was taken from respective authorities. The inclusion criteria of the casts used in this study were fully erupted, non carious and non-worn out mandibular permanent canines in the lower arch, permanent dentition with normal occlusion. The exclusion criteria involved casts with congenitally missing canines, presence of prosthesis, patients with history of orthodontic treatment and malformed canines or canines with developmental defects.

Each parameter of this study was measured separately and independently by two investigators and later values compared to avoid any error. All measurements of the teeth were taken using vernier callipers. The measurements taken were [1] the greatest mesio-distal crown width: - this was measured between the contact points of the tooth on either side of the jaw. Most of the cases showed a bilateral symmetry with this parameter [2], the mandibular canine arch width: this was measured between the tips of both canines in the lower jaw' [4]. There is no statistically significant difference between the right and left mandibular canines amongst males or females so the maximum crown width was considered. Observer error was minimal. In any case if the values differed, a fresh reading was taken by the investigators to ensure accuracy.

The Mandibular Canine Index (MCI) is derived as a ratio between two parameters of permanent mandibular canine teeth, namely the maximum crown width and canine arch width (measured in mm1 and is calculated as follows:

$$MCI = \frac{\text{Mesiodistal crown width of mandibular canine}}{\text{Mandibular canine arch width}}$$

***Corresponding Author**
Email:
christy.e.jacob@gmail.com
Tel.: +91 844 681 0239

IIOAB JOURNAL
ISSN: 0976-3104

RESULTS

The MCI for each subject was calculated as per the formula given above.
The MCI for males have a mean value of 0.284 and for females it is 0.279. Based on these values method of sex predictation from standard value of MCI was derived as follows :

Formula : $\frac{(\text{Mean Male MCI} - \text{SD}) + (\text{Mean Female MCI} + \text{SD})}{2}$

$= \frac{(0.284 - 0.023) + (0.279 + 0.022)}{2} = 0.281$

Standard MCI value obtained : 0.281

This standard value was used and reporting of sex was. All Mandibular Canine Index values up to the limit of the Standard MCI value (0.281) were reported as female. Those values above this limit were reported as male.

The standard value was a base line on which the results were crosschecked and seen if the study proved to be true to determine gender based on the readings.

The accuracy of the method was counter-checked in the graph plotted. The values obtained are presented graphically. A graph was plotted sensitivity vs. specificity and the following reading was obtained. Sensitivity is a reflection of the population number with the expected result and specificity is the measure of the false positive rate.

Variable : MCI Calculated

Disease prevalence unknown.

Area under the ROC curve = 0.556
Standard error = 0.018
95% Confidence interval = 0.525 to 0.587

Table 1: Summarizes the result of sensitivity and specificity obtained from the ROC curve graphically

Criterion	Sens 95% C.I	Spec 95% C.I	+L.R	-L.R
.288	40.6 (36.3-45.0)	70.2 (66.0 – 74.2)	1.36	0.85

Key : Sens = Sensitivity : Sensitivity is the probability that a test will indicate 'disease' among those with the disease[5]
Spec = Specificity: Specificity is the fraction of those without disease who will have a negative test result[5]
+LR = Positive likelihood ratio
-LR = Negative likelihood ratio

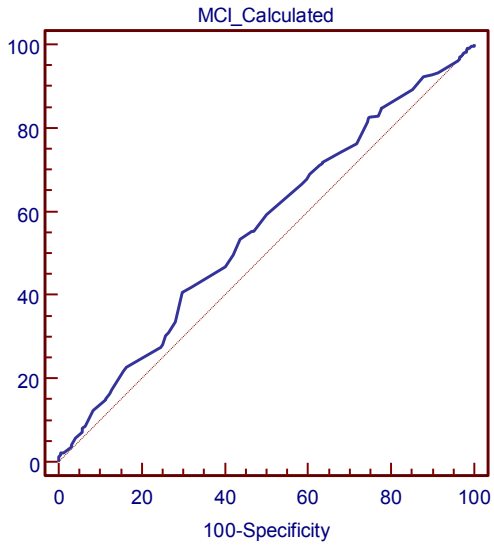

Fig. 1: The data from the table above has been summed in the line graph of specificity vs sensitivity.

IIOAB JOURNAL
ISSN: 0976-3104

Percentage accuracy was then recorded. The percentages were 40.6% in males and 70.2% in females. This proves that males exhibited low accuracy in gender determination using the MCI when compared to females. A wide variation in the percentage was seen between males and females making this index only applicable in females, through this study.

DISCUSSION

Various studies state that the mandibular canine index is an useful and accurate tool in determining the sex of an individual [4-8]. According to a study by Kaushal et al [6], whenever the width of either canine was more than 7 mm, the probability of sex being male was 100. It was seen that with standard MCI, it was possible to detect sex in a North Indian population to as high as 75%. Reddy et al [7] studied the percentage accuracy of sex determination in western Uttar Pradesh and found that males could be predicted correctly in 78% of cases and in females, the accuracy was 66%, so total percentage accuracy was 72%.

However in contradiction few studies state that the mandibular canine index is not an accurate tool for gender determination. The poor ability of the MCI in sex assessment is attributed to it being a relative value–it is obtained as the ratio of two absolute measurements (MD dimension of canines and inter-canine arch width) and does not reflect sex differences that exist in the absolute measurements per say [9,10].

This study done further proves that the MCI is not a reliable source since the values obtained, using the formula and graphically, shows a huge variance and thus cannot be used in the effective determination of sex. Different individuals have different genetic makeup, some females tend to have a larger frame than the others. The same applies with males. Therefore generalizing the overall population and drawing conclusions based on just the width of the canine may not prove to be that accurate a study.

Although, gender determination can be easily done in cases where the cranium is intact. The notable difference between canine in determining sex was noted to be due to the influence of the Y chromosome which was not uniform in all teeth. On the other hand the X-linked genetic influence on tooth width was rather uniform for all teeth [7].

As humans keep on evolving with time, environmental factors play an important role in this evolution. Constantly changing lifestyle, different patterns in diet and early occurrences of growth spurts the results may vary now [10]. Kaushal et al [6] conducted a study back in 1988, stating that the MCI is an important tool for gender determination. But as time progresses, humans evolve, and so does their growth and development. Based on current statistics and casts used for study, we prove that the MCI was more accurate in females who exhibited 70.2%, than males who only exhibited 40.6% accuracy.

Although this method is simple, inexpensive and can be carried out easily, in accordance to our observation, the ability to determine sex is 70.2% in females and 40.6% in males. By comparing the MCI with the standard MCI value will be a profound result found in fragmented female human remains. This method is more accurate and reliable in females due to the percentage of accuracy, when in comparison to males; it did not exhibit even 50% accuracy. But such a method of sex determination has its limitations due to variations of this parameter with geographic distribution. This implies that it is necessary to make up a random sample of the population from this geographical area to calculate the corresponding standard MCI.[11] It can be used just as a supplemental tool in determining the gender of an individual.

CONCLUSION

As it currently stands, MCI does not carry much predictability in the male population as compared to the female. Therefore it may be used as a supplemental tool but it does not carry much relevance to determine the gender. Gender of an individual cannot be estimated if the fragment of the mandible is from the different geographical area unless random sampling of the population of that area has been done to calculate the corresponding MCIs [11]. However, it is not a confirmatory test and is done as an adjunct with other tests for gender identification. Alternative methods should be adopted for gender determination.

CONFLICT OF INTEREST
None

ACKNOWLEDGEMENTS
None

FINANCIAL DISCLOSURE
None

IIOAB JOURNAL
ISSN: 0976-3104

REFERENCES

[1] Girish K, Rahman FS, Tippu SR. [2010] Dental DNA fingerprinting in identification of human remains. J Forensic Dent Sci. 2(2):63-68.
[2] Shamim T. [2012] Forensic odontology. J Coll Physicians Surg Pak. 22(4):240-245.
[3] Vishwakarma N, Guha R. [2011] A study of sexual dimorphism in permanent mandibular canines and its implications in forensic investigations, Nepal Med Coll J. 13(2) : 96-99
[4] Rao NG, Rao NN, Pai ML, Kotian MS. [1989] Mandibular canine index – a clue for establishing sex identity. Forensic Sci Int. 1989, 42(3):249-54.
[5] Lengerich E. STAT 507, Epidemological Research Methods, PennState Eberly College of Science, Pennsylvania, USA (Accessed on May, 2018: https://onlinecourses.science.psu.edu/stat507/)
[6] Kaushal S, Patnaik VV, Agnihotri G. [2003] Mandibular canines in sex determination. J Anat Soc India; 52:119-24
[7] Reddy VM, Saxena S, Bansal P. [2008] Mandibular canine index as a sex determinant: A study on the population of western Uttar Pradesh, J Oral Maxillofac Pathol. 12:56-59.
[8] Singh J, Gupta KD, Sardana V, Balappanavar AY, Malhotra G. [2012] Sex determination using cheiloscopy and mandibular canine index as a tool in forensic dentistry. J Forensic Dent Sci, 4(2):70-74.
[9] Acharya AB, Mainali S. [2009] Limitations of the mandibular canine index in sex assessment. J Forensic Leg Med. 16 (2): 67- 69.
[10] Silva AM, Pereira ML, Gouveia S, Tavares JN, Azevedo Á, Caldas IM. [2016] A new approach to sex estimation using the mandibular canine index. Med Sci Law,56(1):7-12.
[11] Singh SK, Gupta A, Padmavathi B, Kumar S, Roy S, Kumar A. [2015] Mandibular canine index: A reliable predictor for gender identification using study cast in Indian population. Indian J Dent Res, 26:396-399.

IIOAB JOURNAL

ARTICLE

CHANGE IN PHYTOTOXICITY DURING COMPOSTING OF MANURES CONTAINING OXYTETRACYCLINE

Natalya V. Danilova*, Polina Yu. Galitskaya, Svetlana Yu. Selivanovskaya

Department of Applied Ecology, Kazan Federal University, RUSSIA

ISSN 0976-3104

ABSTRACT

Manure from animal farms contains significant amounts of antibiotics, and fertilizers prepared from this manures may contain residuals of antibiotics which are able to suppress soil microbiota and consequently reduce plant growth. Composting is an effective way to reduce the negative impact of antibiotics in manure on the growth of crops. In this paper, we have evaluated the effect of composting on the phytotoxicity of cow manure spiked with various concentrations of OTC (oxytetracycline) (50 mg kg –1, 150 mg kg –1 and 300 mg kg –1). Assessment of phytotoxicity was carried out using oat plants (Avena sativa L.), by contact method on the 1st, 30th, 60th and 90th days of composting. Composts were mixed with soil in a ratio of 1:1, 2:1 and 3:1. It was found that during the first 30 days, all composts had significant toxicity (the germination index did not exceed 10% for any mixtures). Afterwards, phytotoxicity decreased in all the mixtures. On the 60th day, the GI (germination index) ranged from 16.7% to 40.9%, with different OTC concentrations causing significantly differing effects. On the 90th day, the GI (germination index) ranged from 29.3% to 106.6%, with no significant difference observable in the samples with various initial concentrations of OTC. This may be due to decomposition of the antibiotic in the soil.

KEY WORDS
manure, composting, antibiotics, oxytetracycline, phytotoxicity.

Received: 10 May 2018
Accepted: 18 July 2018
Published: 12 Oct 2018

INTRODUCTION

The use of animal manures after composting to restore the fertility of agricultural soils is a common practice for farmers around the world [1]. Composting provides an environmentally friendly approach for the transformation of livestock waste into an effective non–toxic and non–pathogenic organic fertilizer. In the process of composting, the presence of a wide range of complex organic compounds promotes the development of a diversity of microbial communities in the soil which, as a result, stimulate various soil functions [2].

However, the widespread use of antibacterial drugs for the treatment and disease prevention of animals can make the use of manure dangerous due to the risk of spreading antibiotics into soil ecosystems [3,4]. It has been found that up to 90% of the prescribed dose of antibiotics consumed is excreted from the animal's body due to weak absorption in the gastrointestinal tract. Recent studies have shown that manure from livestock farms contains high antibiotic residues at levels from several mg kg –1 or up to several hundreds of mg kg –1 [5]. The most common antibiotics for the treatment of animals are antibiotics of the tetracycline group [5]. Often, untreated animal waste from livestock farms is used to fertilize soils as a raw material [6]. This can create an increasing potential risk for human health, as well as for ecosystems [4]. The use of manure can depress the activity of soil microorganisms and inhibit the natural processes of soil enzyme production [7]. In addition, residues of antibiotics in the composition of manure can pass from the soil into the crops, thereby increasing the risk to human health [8,9]. Such information on the effects of composts contaminated with antibiotics on agricultural plants is, however, scarce. Thus, it is necessary to treat and neutralize this kind of animal waste before using it for soil fertilization [10].

Recently, many studies have shown that composting is an effective method that significantly reduces antibiotics in animal wastes. For instance, Dolliver with coauthors observed the degradation of monensin and tylosin during manure composting and found that the monensin and tylosin was reduced by 54–76% [11]. Rama swamy with coauthors (2010) found that the content of salinomycin decreased by 99.8% over 38 days of composting [10]. According to Arican with coauthors, (2007) the initial level of oxytetracycline decreased significantly by 95% during the first 6 days of composting of cow manure [12]. Such a significant reduction in the content of antibiotics in the manure is most likely facilitated by certain conditions found during composting such as temperature, humidity and various antibiotic biodegradation processes [11,13]. In addition, a decrease in the content of soluble forms of antibiotics may be due to their adsorption on organic components contained in composts. The addition of organic structural agents such as straw and sawdust to manure in compost production can also affect the reduction of antibiotics [6].

The objectives of this paper were as follows: i) to assess the change in phytotoxicity of cow manure containing oxytetracycilne in the process of composting, and ii) to reveal the influence of initial oxytetracycline concentration in the manure of the phytotoxicity dynamics.

METHODS

The object of the study was the manure of cows which had not been treated with antibiotics, selected on a private farm in the Laishevsky District (Republic of Tatarstan). Straw was added to the manure as a structural agent in a ratio 20:6.5 (w/w). Oxytetracycline (OTC) was chosen for the model experiment, since

***Corresponding Author**
Email:
Natalia.Arzhantseva@kpfu.ru

IIOAB JOURNAL
ISSN: 0976-3104

this drug is widely used on livestock in Russia. Three composting mixtures containing 50 mg kg −1, 150 mg kg −1 and 300 mg kg −1 OTC were prepared. As a compost control, a compost mixture without the antibiotic was used. Composts were incubated at room temperature (20–25°C).

The phytotoxicity of the composts was determined on the 1st, 30th, 60th and 90th days of composting by the contact method using oats (Avena sativa L.) as a test object [14]. To do this, composts was mixed with the soil to achieve a 1:1, 2:1 and 3:1 compost–soil ratio. As a soil control, soil without the compost was used. The compost–soil mixtures were moistened up to 60% moisture capacity and maintained at this level throughout the incubation period. Incubation was carried out at room temperature (20-25°C) for 14 days. The germination index (GI,%) was calculated by the formula:

GI (%) = ((Seed germination inn treatment×Root length in treatment))/((Seed germination in control×Root length inn control))×100

RESULTS

Phytotoxicity of composts is one of the often measured parameters characterizing the maturity of composts, and therefore their suitability for safe soil fertilization. This method is based on the evaluation of the effect of compost applied to the soil on the intensity of germination of seeds and the early stages of growth of a number of plants [15]. In this paper, the phytotoxicity of composts contaminated with OTC was investigated using oat (Avena sativa L.) seeds.

In the first stage, the phytotoxicity of compost–soil mixtures, prepared with manure from cows not containing antibiotics, was analyzed. The results of the estimation of the germination index of the oat seeds (Avena sativa L.) are shown on the [Fig. 1].

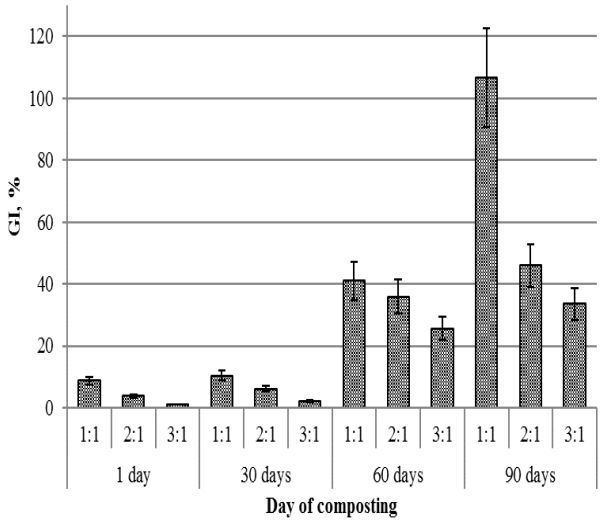

Fig. 1: Change in phytotoxicity in the process of composting of manure not contaminated with antibiotics.

As can be seen from the [Fig. 1], in the first 30rd days of the composting process, all mixtures of soil and compost from manure that did not contain antibiotics had high toxicity. The germination index in this case did not exceed 10%. A correlation was found between the degree of phytotoxicity and the amount of compost mixed with the soil: the higher the compost content, the stronger the inhibitory effect on oat growth. On the 60th day of the composting, the germination index increased to 40.9%, 35.9% and 25.6% in the compost–soil mixtures 1:1, 2:1 and 3:1, respectively. On the 90th day in 1:1 ratio mixture of compost and soil, the germination index was 106.6%, which is 2.6 times higher than that on the 60th day. In mixtures with compost–soil ratios of 2:1 and 3:1, phytotoxicity remained almost unchanged from its level on the 60th day of composting. In general, a trend was observed indicating the reduction of phytotoxicity in compost with the passage of time.

In the second stage of the study, the phytotoxicity of mixtures from soil and compost contaminated with various concentrations of OTC was assessed. The results are shown in [Fig. 2].

IIOAB JOURNAL
ISSN: 0976-3104

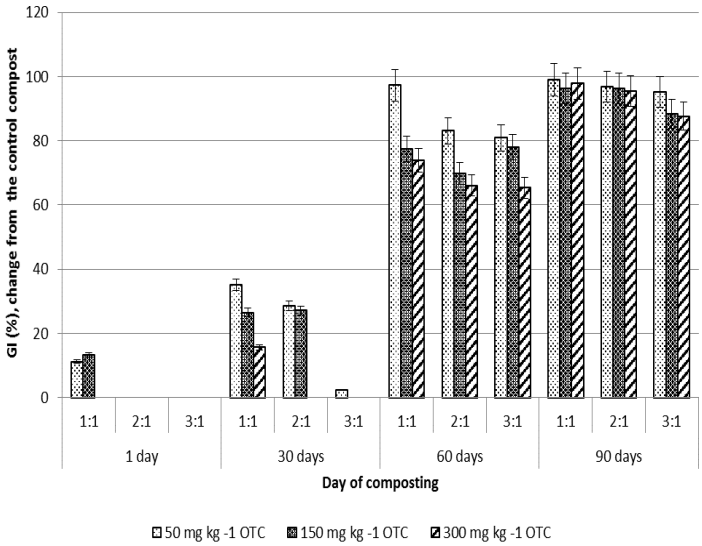

Fig. 2: Change in phytotoxicity in the process of composting of manure containing different concentrations of OTC.

As can be seen from the [Fig. 2], there were similar dynamics in the change in toxicity in the process of composting of manures contaminated with OTC. During the first 30 days of the composting process all the compost–soil mixtures were characterized by a high level of toxicity.

On the 30th day in the mixture 1:1 there were significant differences in the GI between different concentrations of OTC. On the 60th day there was a decrease in the level of phytotoxicity for all composts. However, significant differences were found between the toxic effects of composts with different initial antibiotic content. The germination index decreased with increasing dose of OTC in the manure. The difference of GI from the control compost without OTC was on average 76.8%.

On the 90th day it was found that all the composts from the contaminated manure had equally low toxicity levels as the control compost. The change of GI from the control compost without OTC was on average 94.7%. Interestingly different concentrations of oxytetracycline added to manure before composting did not cause significant differences to the level of phytotoxicity.

DISCUSSION

Animal wastes from farms in raw form contain many toxic compounds that are harmful for plants [1]. Therefore, in the early stages of composting, compost is not commonly suitable for healthy plant growth [16]. The current study has showed results that are in close agreement with previous studies investigating the phytotoxicity of compost. Thus, in the initial stages (first 30 days) of composting of cow manure not containing antibiotics, high toxicity was observed, and toxicity was higher in the mixtures with a greater proportion of compost. By further observation of the composting process, the trend towards a reduction in the toxicity of the compost was revealed. It is known that in the process of composting, the original manures loses its harmful components, which is demonstrated by the fact that, when used as a fertilizer, such composts are able to create favorable conditions for plant growth [1]. In our study, toxicity continued to reduce up to the 90th day in the 1:1 mixture of compost and soil.

Manure from livestock contains a large quantity of antibiotics and there is a risk of their spread in the terrestrial and aquatic environments [4]. Composting is an effective way to reduce residues of antibiotics in animal waste from farms [17]. Many studies have demonstrated that manure loses its pathogenic properties, the many poisonous substances for plants, in the composting process and, consequently, it is effective in reducing the toxic effect on plant growth [6,10]. During the initial stages of composting, manure contaminated with OTC had the same high toxicity as those in the non–contaminated samples. However, the absence of additional OTC effect may be due to high toxicity of the compost mixtures themselves. On the 30th day of the composting process, there were significant differences in the level of toxicity between samples containing different concentrations of OTC. The association between increased toxicity and increased concentration of OTC in manure was noted. Therefore, the presence of antibiotics in the manure can affect the compost in a way which has increased the toxicity for plants. On 60th day the composts continued to have a toxic effect on oat plants. In addition, significant differences in the level of toxicity in composts containing different initial concentrations of OTC were found. It appears that, for this composting period (60 days), residual OTC concentrations can have a direct toxic effect on the growth and development of oat plants. Many studies also confirm the fact that when present in the composting process, antibiotics contained in the initial manure have a direct toxic effect on plants [18–20]. In addition, the presence of OTC in the manure could inhibit the microbial communities within the compost

IIOAB JOURNAL
ISSN: 0976-3104

that drive the composting process. Thus, inhibition of microbial communities could inhibit the composting process itself, and, consequently, create a natural decrease in phytotoxicity [17]. Many studies also provide conclusions explaining the indirect effect of antibiotics on the toxicity of composts due to the deceleration of the composting process caused by the inhibition of the functioning of microbial communities [1,9,17].

On the 90th day of the composting process, composts had low toxicity towards oat plants. At this stage of the composting process, there was no difference in the level of the toxicity of composts with different amounts of antibiotic. It is likely that the decrease in the toxicity at the end of the composting process is due to the gradual decomposition of OTC in composting mixtures. Our previous study found that the destruction of OTC when added to the soil occurs at a level of 98% after a 35 days incubation period [21]. Other works also indicate the gradual destruction of antibiotics in soil and manure [10,11,22].

SUMMARY

In this work, an assessment of the change in phytotoxicity in the composting of manure, both pure and containing antibiotics was conducted. It showed a regular decrease in the toxicity of compost, from manure that does not contain antibiotics over the composting period. On the 60th day of composting, the germination index increased to 40.9%, 35.9% and 25.6% in the 1:1, 2:1 and 3:1 compost and soil mixtures, respectively. On the 90th day in the 1:1 mixture of compost and soil, the germination index was 106.6%, which is 2.6 times higher than in the same mixture the 60th day. By the end of composting (90 days), composting mixtures containing manure contaminated with oxytetracycline, also showed a reduction in toxicity. The lowest levels of phytotoxicity at the end of composting were found in soil and compost mixtures in a 1:1 ratio regardless of the presence of the antibiotic in the original manure.

CONCLUSION

The results of this study showed that in the early stages of composting, composts, from both pure manure and from those contaminated with antibiotic had a significant level of phytotoxicity. The most rapid decrease in phytotoxicity occurred in compost prepared with pure manure. At the end of composting, the different initial concentrations of oxytetracycline in the manure did not cause significant differences in the level of phytotoxicity. However, in the process of composting (day 60), initial antibiotic concentration did play a role in the compost toxicity.

CONFLICT OF INTEREST
There is no conflict of interest.

ACKNOWLEDGEMENTS
This work was performed with the financial support of a subsidy allocated to Kazan Federal University from Russian Foundation for Basic Research, project No 16–04–00443. The work is published with support of the Russian Government Program of Competitive Growth of Kazan Federal University.

FINANCIAL DISCLOSURE
None

REFERENCES

[1] Bernal MP, Alburquerque JA, Moral R. [2009] Composting of animal manures and chemical criteria for compost maturity assessment. A review, Bioresour Technol. 100(22):5444–5453.
[2] Liu B. et al. [2015] Effects of composting process on the dissipation of extractable sulfonamides in swine manure, Bioresour. Technol. 175: 284–290.
[3] Kemper N. [2008] Veterinary antibiotics in the aquatic and terrestrial environment, Ecol Indic. 8(1):1–13.
[4] Sarmah AK, Meyer MT, Boxall AB. [2006] A global perspective on the use, sales, exposure pathways, occurrence, fate and effects of veterinary antibiotics (VAs) in the environment, Chemosphere. 65(5):725–759.
[5] Wu X. et al. [2011] The behavior of tetracyclines and their degradation products during swine manure composting, Bioresour Technol. 102(10):5924–5931.
[6] Kim K, et al. [2012] Decline in extractable antibiotics in manure-based composts during composting, Waste Manag. 32:110–116.
[7] Thiele-Bruhn S. [2003] Pharmaceutical antibiotic compounds in soils A review, J Plant Nutr Soil Sci. 166(2):145–167.
[8] Pan M, Chu LM. [2017] Fate of antibiotics in soil and their uptake by edible crops, Sci Total Environ. 599–600:500–512.
[9] Tasho RP, Cho JY. [2016] Veterinary antibiotics in animal waste, its distribution in soil and uptake by plants: A review, Sci Total Environ. 563–564(3):366–376.
[10] Ramaswamy J, et al. [2010] The effect of composting on the degradation of a veterinary pharmaceutical, Bioresour Technol. 101(7):2294–2299.
[11] Dolliver H, Noll SL. [2008] Antibiotic degradation during manure composting, J Environ Qual. 37:1245–1253.
[12] Arikan OA, et al. [2007] Composting rapidly reduces levels of extractable oxytetracycline in manure from therapeutically treated beef calves, Bioresour. Technol. 98(1):169–176.
[13] Chen GX, et al. [2014] Effect of different oxytetracycline addition methods on its degradation behavior in soil, Sci Total Environ. 479–480(1):241–246.
[14] [2005] ISO 22030:2005 Soil quality Biological methods — Chronic toxicity in higher plants. 18.
[15] Luo Y, et al. [2017] Seed germination test for toxicity evaluation of compost: Its roles, problems and prospects, Waste Manag. in press.
[16] Tiquia SM. [2010] Reduction of compost phytotoxicity during the process of decomposition, Chemosphere. 79(5):506–512.
[17] Selvam A, Zhao Z, Wong JWC. [2012] Composting of swine manure spiked with sulfadiazine, chlortetracycline and ciprofloxacin, Bioresour Technol. 126:412–417.

IIOAB JOURNAL
ISSN: 0976-3104

[18] Bártíková H, Podlipná R, Skálová L. [2016] Veterinary drugs in the environment and their toxicity to plants, Chemosphere. 144:2290–2301.
[19] Ghava K, Rathod MC, Dhale DA. [2015] Effect of antibiotics on seed germination and root elongation of wheat, Int J Curr Microbiol App Sci. 4(1):516–527.
[20] Hillis DG, et al. [2011] Effects of ten antibiotics on seed germination and root elongation in three plant species, Arch Environ Contam Toxicol. 60(2):220–232.
[21] Danilova N, Galtskaya P, Selivanovskaya S. [2018] Veterinary antibiotic oxytetracycline influences the soil microbial community even after its decomposition, Eur J Soil Sci in press.
[22] Ho Y, Bin et al. [2013] Degradation of veterinary antibiotics and hormone during broiler manure composting, Bioresour Technol. (131):476–484.

ARTICLE

GENETIC POLYMORPHISM OF VASCULAR SYSTEM, DYSFUNCTION OF THE ENDOTHELIUM AND THE BLOOD COAGULATION SYSTEM AMONG WOMEN WITH GESTOSIS (PREECLAMPSIA)

Tatiana V. Pavlova*[1], Larisa I. Maltseva[2]

[1]*Dept. of Obstetrics, Kazan Federal University, Medical Sanitary Unit of FSAEI HE, Kazan, RUSSIA*

[2]*Dept. of Obstetrics and Gynecology, Kazan State Medical Academy, Kazan, RUSSIA*

ISSN 0976-3104

ABSTRACT

The article presents the results of a study to determine the genetic risk of pre-eclampsia in primiparous women. We have examined 165 primiparous women: 75 pregnant women with different degrees of severity of preeclampsia; 40 ones from the high-risk group, 50 - practically healthy primiparous women. The examination has shown that the determination of genetic defects, the level of folic acid, angiotensin-converting enzyme, renin, angiotensin, intravascular coagulation markers is prognostically significant in the diagnosis of severe preeclampsia, premature detachment of the normally located placenta, placental insufficiency, syndrome of retarded fetal development and congenital malformations of fetus in primiparous women.

KEY WORDS
gestosis, preeclampsia, genetic polymorphism, endothelial dysfunction, folate deficiency, hyperhomocysteinemia

Received: 8 May 2018
Accepted: 19 July 2018
Published: 12 Oct 2018

***Corresponding Author**
Email:
Maria.Pavlova@kpfu.ru

INTRODUCTION

Gestosis (preeclampsia) is one of the topical problems of modern obstetrics and remains the most severe complication of pregnancy. The frequency of preeclampsia does not tend to decrease and fluctuates in Russia from 7% to 29% [1, 2], largely determining the indicators of maternal mortality and infant morbidity rate [3, 4]. According to recent studies, the genetic predisposition to the development of preeclampsia may be up to 50% of all risk factors [5, 6, 7]. The genetic factors with which preeclampsia may be associated include: metabolic genes (GSTM1, GSTT1, GSTP1, EPHX, CYP1A1); the main histocompatibility complex (HLA-G, DQA1, DQB1, DRB1); blood coagulation systems (FV, FII, MTHFR, FGB, ITGB3, F7); endocrine system (ESRI, ESRII, INHA); lipid metabolism (LPL, APOE, PPARG, ADRB3); cytokines and growth factors (TNFA, IGFI, IL1Q, ILIA, IL1B, IL1RN, CTLA4); endothelium (NOS3, EDNI, GNB3, VEGF); vascular system (ACE, AGT, REN, AGTR1, AGTR2, PAI 1). The products of the genes of the renin-angiotensin system are among the most important regulators of blood pressure and the homeostatic function of the kidney, ensuring the maintenance of vital processes in the body.

In recent years, the existence of variants of the gene of the angiotensin-converting enzyme (ACE) has been discovered. The ACE gene is mapped on chromosome 17q23. When cloning the ACE gene, it has been revealed that either Insertion (I) is comprehended or Deletion (D) Alu repeat, consisting of 287 base pairs is absent in Intion 16 [8, 9]. The level of ACE in serum in the patients who are homozygous for D alleles exceeded almost twice the level of the enzyme in homozygous for I alleles and has an average value in heterozygous - I/D genotype [9, 10]. The angiotensinogen gene (AGT) is located on the long arm of the 1st chromosome at the locus Iq42-q43. The plasmatic level of angiotensinogen reflects its level of expression. The most studied are the M235T and T174M variants of the AGT gene. The association of the T-allele and the T/T genotype with high blood pressure is for the M235T variant (replacement of methionine by threonine) [9, 11]. Polymorphism of the gene for angiotensin converting enzyme (ACE) and angiotensinogen (AGT) is poorly related to the frequency and course of chronic arterial hypertension (CAH) without pregnancy, but may be a risk factor for the development of hypertension in pregnant women.

The main endothelial factor of relaxation is nitric oxide (NO). It is involved in maintaining the tone of the vascular wall, thrombo genesis, neurotransmission, immune system reaction, etc. [8,10]. Currently, three isoforms of NOS have been identified: NOS1 - neuronal (nNOS) or brain (bNOS); NOS2 - inducible (iNOS) or macrophage (mNOS); NOS3 - endothelial (eNOS) [12]. Each of them has features in the mechanisms of action, localization, in the biological significance for the organism. In the endothelium, thrombocytes, arterioles, mesangial cells, etc. eNOS is localized in large quantities [8]. The allelic variants of this gene lead to decrease of the level of expression of NO-synthetase and, as a result, diminution of the organism's resistance to hypertensive states from the external and internal environment.

From the genes of the blood coagulation system, the most extensively studied is the polymorphism of the gene of methylenetetrahydrofolate reductase MTHFR. Two variants of the gene have been described, the most significant of which is the mutation of C677T. The individuals being homozygous for this mutation have the thermo ability of MTHFR and the reduced enzyme activity to about 35% of the mean value. This mutation is accompanied by an increase of the level of homocysteine, which is a risk of pre-eclampsia in pregnant women. Over frequency of the 677T allele was observed not only with preeclampsia, but also with other complications of pregnancy (placental abruption, fetal growth retardation, antenatal death of fetus, fetal neural tube defects). Another important aspect of the MTHFR-C677T mutation is folate-deficiency anemia,

IIOAB JOURNAL
ISSN: 0976-3104

which further aggravates hypoxia, the course of disseminated intravascular coagulation and, thereby, contributes to the progression of microcirculatory disorders and the aggravation of preeclampsia [13, 14].

Obviously, preeclampsia has a number of genes of predisposition, so identifying candidate genes for the development of preeclampsia can help in defining a risk group and conducting effective prevention of this severe pathology. Especially unpredictable pre-eclampsia is in primiparous women and its relationship with genetic factors is extremely interesting.

In connection with this, we conducted a study which aimed to determine the polymorphism of a number of genes of the vascular system, endothelial dysfunction and the system of blood coagulation and their role in the development of preeclampsia in primiparous women.

MATERIALS AND METHODS

We have examined 165 primiparous women in the 27-38 weeks of their pregnancy at the age of 25,4 ± 5,43 years: 75 pregnant women with different severity of preeclampsia (50 - with moderate degree, 25 - severe), 40 women without a pre-eclampsia clinic, but from the group of high risk (with obesity - 10, with hypertension before pregnancy - 10, with kidney disease - 20) and 50 practically healthy pregnant women. Written informed consent was taken from all the participants and the study was approved by the Institute ethical committee, Commission of the Department of the Obstetrics.

All the patients have had, in addition to general clinical checkup with assessment of the hemostasiogram (platelet aggregation: spontaneous and induced, fibrinogen, APTT, INR, XIIa dependent fibrinolysis, AT III, FMSC, PDP, plasminogen, protein C and S), the blood tested by the method of PCR in real-time on detection of the polymorphism of the genes AGT-M235T (angiotensinogen), ACE I / D (angiotensin converting enzyme), MTHFR-C677T (methylenetetrahydrofolate reductase), E298D polymorphism by restriction analysis and 4a / 4b polymorphism in the NOS3 gene. The gene NOS3-E298D, 4a / 4b is responsible for the synthesis of the enzyme – endothelial NO synthase (eNOS), which participates in the synthesis of nitric oxide by endothelium and, consequently, in the regulation of vascular tone, blood flow and blood pressure. The studied genes were assessed with all variants of their mutations (AGT-T235T, ACE D / D, MTHFR-T677T, NOS3-D298D, 4a / 4a). The level of folic acid (FA), angiotensin-converting enzyme (ACE) and renin-angiotensin (RA) was determined by the method of immune chemiluminescent analysis (ICA).

The standard method χ^2 was used for statistical analysis. In the case of a small quantity or absence of any genotypes (alleles), the exact two-sided Fisher test recommended for such situations was used to verify the reliability of the differences obtained. The relative risk (odds ratio - OR) of disease development in a particular genotype was calculated according to the standard formula OR = ad/bc, where a and b are the number of patients with and without a mutant genotype, respectively, and c d are the number of women in the control group also having and not having a mutant genotype. OR is indicated with a 95% confidence interval. To calculate the comparison of the average values of digital data, as well as to verify the reliability of the results obtained, we used the methods of estimating the difference between parts, analysis of average trends (t – Student's test), correlation analysis. The level of $p < 0,05$ was taken for the reliability of the differences.

RESULTS

As shown by the studies, among healthy primiparous women, normal variants of the studied genes are determined in 98% of cases [Table 1]. In 2% of pregnant women, single mutant variants of the genes AGT-T235T, ACE D / D, NOS3-D298D, 4a / 4a were established, which were not realized in obstetric pathology. The measures of RA, ACE in this group were within the norm (1,7 ± 0,3, 3,3 ± 1,2 and 38,89 ± 25,34, respectively). The level of FA was reduced by 15% in 16 pregnant women and averaged 8,45 ± 4,51 ng / ml [Table 2].

Practically all obese pregnant women are in the risk group, 8 out of 10 have a mutant version of MTHFR-T677T with a slight decrease in FA and an increase in ACE. One of them had, at the same time, a small malformation of the fetus (non-closure of palate – cleft palate). A mutant variant of MTHFR-T677T was also detected in 7 out of 10 women with hypertensive syndrome, one of them - in combination with a mutant variant of the ACE D / D gene and a slight increase in the level of CR. -A mutant variant of the ACE D/D gene and polymorphism of the NOS3-E298D, 4a/4b gene, where the alleles D and 4a raise the risk of preeclampsia, placental insufficiency, FGRS, with potentiating factors was disclosed in 10 women with pyelonephritis. Such factors could be a two-fold elevation of renin and angiotensin with a simultaneous decrease in FA by 1,8 times, which were found in these women. On average, a significant decrease in folic acid with increased renin, angiotensin and ACE was found in at-risk pregnant women with developing pre-eclampsia in comparison with healthy pregnant women [Table 2]. Attention was drawn to the absence of changes in haemocoagulative parameters.

During the assessment of pregnant women with moderately expressed pre-eclampsia, mutant genes of MTHFR-T677T in 38% of cases (19 women) and ACE D / D in 46% (23) were revealed, a combination of these mutant variants was found in two patients. The heterozygous variant of MTHFR-C677T was determined in a third of the primiparae of this group, which was clinically realized in placental insufficiency

IIOAB JOURNAL
ISSN: 0976-3104

and in the Syndrome of fetal growth retardation of I-II intensity in 7 pregnant women. Nine women with a mutant variant MTHFR-T677T had also FGRS of II intensity, long-lasting intrauterine hypoxia, oligohydramnios, at the same time, one of them had a partial detachment of the normally located placenta at 37 weeks pregnancy. The normal variant of the MTHFR-C677C gene was detected in 32% (16 pregnant women). The mutant gene for the D-NOS3-D298D, 4b / 4b allele was found in 30% (15 patients), all of them had clinical FGRS hypamnion. In the haemostasiogram of women with mild pre-eclampsia having mutant genes, an increase in D-dimer, fibrinogen, plasminogen, decrease in AT-III were revealed, i.e. manifestations of the syndrome of DIC.

Table 1: The results of the study the Allele frequencies of the polymorphic variants studied

Subjected groups	Evaluated polymorphism														
	MTHFR-C677T			ACE-I/D			AGT-M235T			eNOS-E298D			eNOS-4a/4b		
	CC	CT	TT	II	ID	DD	MM	MT	TT	EE	ED	DD	bb	ab	aa
Healthy pregnant women (n=50)	0,6*	0,33*	0	0,35*	0,54	0,11*	0,73*	0,27*	0	0,86*	0,24*	0	0,7	0,3*	0
Pregnant women at risk of preeclampsia (n=40) of them:	0,2*	0,18*	0,54*	0,6*	0,23*	0,17*	0,62*	0,38*	0	0,46	0,54*	0	0,6*	0,4*	0
With obesity (n=10)	0,1*	0,1*	0,8*	0,7	0,3*	0	0,6*	0,4	0	0,5*	0,5	0	0,7*	0,3*	0
With hypertensive syndrome (n=10)	0,2*	0,1*	0,7*	0,8*	0,2*	0	0,9	0,1*	0	0,4*	0,6*	0	0,6*	0,4	0
With renal diseases (n=20)	0,5*	0,45*	0	0,3*	0,2	0,5*	0,35*	0,65*	0	0,5	0,5*	0	0,5	0,5*	0
The group with moderate preeclampsia (n=50)	0,2*	0,34*	0,38*	0,3*	0,24*	0,46	0,34*	0,48	0,66*	0,5	0,2*	0,3*	0,44*	0,54*	0,02*
The group with severe preeclampsia (n=25)	0,08*	0,12*	0,8*	0,32*	0,24*	0,56	0,4*	0,32*	0,28	0,28*	0,4*	0,32*	0,12*	0,24*	0,64*

Note: n – the number of individuals in a group, *- accuracy of allele frequencies by comparing the subjected groups with a control group (p<0,05)

Table 2: The level of Folic Acid, Angiotensin-Converting Enzyme, Renin-Angiotensin in the studied groups

Subjected groups	FA, ng/ml	ACE, U/l	Renin, ng/ml/h	Angiotensin, ng/ml
Healthy pregnant women (n=50)	8,45±4,51*	38,89±25,34*	1,7±0,3*	3,3±1,2*
Pregnant women at risk of preeclamsia (n=40)	6,15±2,51*	55,46±18,14	2,54±1,27*	5,01±2,75*
Pregnant women with moderate preeclamsia (n=50)	3,08±1,64*	71,01±21,04*	4,54±2,27*	8,03±2,79*
Pregnant women with severe preeclamsia (n=25)	2,37±1,12**	89,99±24,01*	6,21±2,8*	10,64±3,66*

Note: n – the number of individuals in a group, *- accuracy of allele frequencies by comparing the subjected groups with a control group (p<0,05)

The majority of pregnant women with severe preeclampsia – 73,2% (18) had a combination of mutant gene variants: 56% of them had ACE D/D and MTHFR-T677T (14). In 9 of them, a mutant variant of the AGT-T235T gene was also disclosed [Table 1]. In one woman, mutation of MTHFR-T677T was clinically realized in premature detachment of the normally situated placenta at pregnancy of 27 weeks. In this group, there was also a significant increase in ACE (89,99 ± 24,01), a triple increase in D-dimer values, hyperfibrinogenemia, expressed thrombocyte hyper-aggregation, decrease in AT-III, which corresponded to the active DIC syndrome.

Women with severe preeclampsia in 65% [16] had a mutant variant of the gene for allele 4a –NOS3-4a/4a. This was accompanied by early edema, proteinuria, as well as an active course of DIC syndrome. In 36% [9], the homozygous form of D298D polymorphism of the NOS3 gene was established [Table 1]. In this case, the FVRS of II - III with the progressive increase in the severity of preeclampsia was clinically defined.

IIOAB JOURNAL
ISSN: 0976-3104

Statistical analysis confirmed that NOS3-D298D and NOS3 4a/4a genotypes are significantly more frequent in women with preeclampsia than in patients at risk (χ^2 = 5.81, p <0,05 and χ^2 = 6,03, p <0,05, respectively).

The results of our studies have shown that the presence of the mutant variant of the gene for the allele 4a – NOS3-4a/4a is always accompanied by earlier edema, proteinuria and, as a rule, the formation of FGRS of severity II-III. The highest level of basal NO corresponds to genotype 4b/4b, whereas the level of NO was 2 times lower in women with genotype 4a / 4a. Heterozygous mutation forms occupy an intermediate position in terms of NO. Association 4a/4a of the genotype of the NOS3 gene with the development of preeclampsia made it possible to estimate the relative risk of this complication in pregnant women as significant – 1,74 (CI-95%: 1,06-2,97).

A comparative analysis of the polymorphism of the ACE I/D gene has shown that the DD genotype in women with preeclampsia is found 6,1 times more often (48,8%) than in healthy women (8%). In severe cases, the genotype of DD is found in 36% of pregnant women (χ^2 = 4,82, p <0,05). In the ACE I/D polymorphism, the presence of D allele is associated with the development of preeclampsia (OR 2,15 and CI 95%: 0,77-5,27) and should be considered as a risk factor of the development of preeclampsia, whereas in the analysis of frequencies of genotypes and alleles of AGT -M235T in all groups, significant differences are not revealed.

According to the indication of genetic diversity - PIC (informational content of polymorphism), which gives an idea of how informative the selected marker is, all the studied genetic parameters (I/D, M235T, E298D, 4a/4b, C677T) turned out to be moderately informative (0,319; 0,331; 0,366; 0, 316, respectively), which proves their role in the development of pre-eclampsia in primiparous women.

DISCUSSION

The reasons for the development of preeclampsia in women during pregnancy remain unclear and much attention to the development of the genetic mechanisms of this complication of pregnancy is understandable.

It is quite obvious that pre-eclampsia is a polygenic pathology. A lot of data on the expression of various genes, encoding ACE, angiotensin, endothelin, synthycin 1 and 2, involved in stimulating the cytotrophoblast cells migration and placenta development, endothelial vascular growth factor, methylenetetrahydrofolate reductase, etc. There are data on changes in HLA antigen alleles as the cause of pre-eclampsia development [3, 10]. Of particular interest are primiparous women who do not have a severe obstetrical anamnesis, and that is why they are related to an unpredictable category of patients, as well as at-risk women - with obesity, hypertension, renal diseases.

The results of our studies have shown that both primiparous women with preeclampsia and a group of high-risk development have common genetic changes. A mutant variant of the MTHFR-T677T gene was found in pregnant women with obesity and hypertensive syndrome (80%). The patients with pyelonephritis had the mutant variant ACE D/D dominated, which gives the most severe course of preeclampsia. The rest had heterozygous variants of AGT-M235T, NOS3-E298D, 4a/4b and single variants of their mutations.

Preeclampsia of moderate severity was accompanied by a mutant MTHFR-T677T gene in 38% of cases and ACE D/D in 46%, a heterozygous variant was found in every third pregnant woman, in combination with placental insufficiency and FGRS. The mutant variant of the gene of the D –NOS3 D298D allele leads to similar complications.

Most women with severe preeclampsia have a combination of mutant ACE D/D genes, MTHFR-T677T, and a mutant variant of the AGT-T235T gene is revealed in 50%. In addition, in severe form, as a rule, a mutant variant of the gene of the allele 4a–NOS3 4a/4a with an early onset and progressive increase in severity is identified. It should be noted that the changes in the genetic portrait of women with preeclampsia were probably defined by other equally severe obstetric complications - FGRS in 46%, chronic fetoplacental insufficiency with fetal hypoxia in 33%. Also, the mutation in the MTHFR gene in two cases was clinically accompanied by a partial detachment of the normally situated placenta at pregnancy of 27 and 37 weeks.
It is important to emphasize that the mutation of the studied genes in pregnant women with preeclampsia has always been combined with an abrupt decrease in the level of FA (by 60-80% of the norm) and a significant increase in RA [Table 2].

As it turned out, the decrease in values of FA with the normal variant of the MTHFR-C677C gene during pregnancy does not lead to the development of hypertensive syndrome, but is realized by a greater frequency of placental insufficiency and FGRS.

A low level of FA with an increase in RA against the background of the expression of mutant genes is accompanied by a disruption in the system of hemostasis and hypertensive syndrome of varying severity. The initial signs of DIC syndrome were observed with moderate severity of preeclampsia, progressive DIC syndrome - with severe course.

IIOAB JOURNAL
ISSN: 0976-3104

However, assessment of changes in the parameters of folic acid, ACE, renin and angiotensin requires special attention. A significant correlation between the level of FA, ACE, renin, angiotensin and the severity of preeclampsia ($r = -65$; $r = 0,57$; $r = 72$; $r = 0,68$, respectively; $p < 0,05$) was found.

The data obtained have shown that the decrease in FA with increasing ACE, renin, angiotensin is observed in women at risk and with the increase in the severity of preeclampsia, the values of FA progressively decrease by 60-80% of the norm, while the values of ACE, renin, and angiotensin increase 1,6; 2,5 and 2 times, respectively, compared with women at risk [Table 2].

Probably the mutant MTHFR genes found in women at risk and in those ones with preeclampsia lead to an imbalance of folate metabolism and even the prescription of synthetic folic acid is unable to change the situation with folate deficiency and the formation of endotheliopathy. The mutant genes of renin, angiotensin, nitrous oxide increase endothelial dysfunction with the development of vascular complications and severe obstetric syndromes.

Thus, the detection of genetic defects, the levels of folic acid, ACE, renin, angiotensin, and intravascular coagulation markers can be prognostically significant in the diagnosis of severe pre-eclampsia, premature detachment of the normally located placenta, placental insufficiency, FGRS and fetal malformations in primiparous women, who do not have a burdened obstetrical anamnesis.

CONCLUSION

The development of pre-eclampsia in primiparous women is genetically determined. Polymorphism of the genes of nitrogen oxide – NOS3-E298D, 4a/4b, mutation in gene of angiotensin converting enzyme – ACE D/D with pyelonephritis, mutation in gene of methylene tetra hydro folate reductase – MTHFR-T677T with chronic hypertensive states and obesity form a risk group of women with a high potential for realization in preeclampsia. The development of mild pre-eclampsia is determined by the mutation of one of the genes: MTHFR-T677T, ACE D/D, or NOS3-D298D, 4a/4a, combined with a 60% decrease in folate levels and a 2-fold elevation of the ACE in blood in pregnant women. A severe form of pre-eclampsia occurs with a combined mutation of MTHFR-T677T and ACE D/D or the presence of the NOS3-D298D, 4a/4a genes with reduced folate content by 80% compared to healthy primiparae and an increase in ACE by more than 2 times.

CONFLICT OF INTEREST
There is no conflict of interest.

ACKNOWLEDGEMENTS
The work is performed according to the Russian Government Program of Competitive Growth of Kazan Federal University.

FINANCIAL DISCLOSURE
None

REFERENCES

[1] Radzinsky VE. [2004] Immunologic and Genetic Predictors of Gestosis and FGRS. Materials of the 36-th Annual Congress of International Society on Pathophysiology of Pregnancy of Organization of Gestosis. 187-188.
[2] Radzinsky VE, Orazmuradov AA, Knyazev SA, et al. [2006] Reduction in Obstetric Aggression with Pregnancy of Low perinatal Risk Herald of Russian University of Peoples' Friendship, series Medicine. 4:5-12.
[3] Ailamazyan EK, Mozgovaya EV. [2008] Gestosis Theory and Practice. M Medpress Inform. 271.
[4] Radzinsky VE, Kuznetsova OA, Aleyev IA, et al. [2006] Controversies in Obstetrics (Obstetrics Roundup. «The 7th world congress on controversies in obstetrics, gynecology and infertility». Athens. Greece, 2005) Obstetrics and Gynaecology. 2:59-62.
[5] Ginter EK. [2006] Medical Genetics Textbook. M Medicine. 131-141.
[6] Mozgovaya EV. [2003] Estimate of Genetic Predisposition to Gestosis: Polymorphism of Genes in Regulation of the Function of Endothelium. Journal of Obsterics and Diseases of Women. 3(2): 25-34.
[7] Ness RB, Roberts JM. [2006] Heterogeneous causes constituting the single syndrom of preeclampsia: A hypothesis and its implications. Am. J. Obstet. Ginekol. 175:1365-1370.
[8] Strizhakov AN, Bayev OR, Ignatko IV. [2006] Prediction of Gestosis Development and Feto placental Insufficiency. Russian Journal of Obstetrician Gynecologist. 1:39-42.
[9] Arngrimsson R, Hayward C, Nadaud S. [1997] Evidence for a familial pregnancy-induced hypertension locus in the eNOS-gene region Am J Hum Genet. 61:354-362.
[10] Cooper DW. [2007] Genetikcs of Hypertension in pregnancy: possible single gene control of preeclampsia and eclampsia. Am J Obstet Ginekol. 53: 851-863.
[11] Ookif Takakuwa K, Akashi M, et al. [2008] Am J Reprod. Immunal. 60(1):75 – 84.
[12] Frost P, Blom H, Milos R, et al. [2005] A candidate genetic risk factor for vascular disease: a common mutation in methylenetetrahydrofolate redyctase Nat. Genet. 10:111-113.
[13] Zhou N, Chen J, et al. [2004] Detection of insertion deletion polymorphism of angiotensin converting enzymegene in preeclampsia. Zhonghua Yi Xue Yi Chuan Xue Za Zhi. 16(1):29-31.
[14] Williams MA, Sanchez SE, et al. [2004] Methylenetetrahydrofolate redyctase 677 C T polymorphism and plasma folate in relation to preeclampsia risk among Peruvian women. Matern. Fetal Neonatal Med. 15:337-344.

IIOAB JOURNAL

ARTICLE

A COMPARATIVE STUDY ON SEGMENTATION AND CLASSIFICATION IN BREAST MRI IMAGING

Ahmet Haşim Yurttakal[1*], Hasan Erbay[2], Türkan İkizceli[3], Seyhan Karaçavuş[4], Gökalp Çinarer[1]

[1]*Computer Technologies Department, Bozok University, Yozgat, TURKEY*

[2]*Computer Engineering Department, Kırıkkale University, 71450, Kırıkkale, TURKEY*

[3]*Department of Radiology, University of Health Sciences, Istanbul, TURKEY*

[4]*Department of Nuclear Medicine, University of Health Sciences, Kayseri, TURKEY*

ISSN 0976-3104

ABSTRACT

Background: *Breast cancer is the type of cancer that develops from cells in the breast tissue. The breast cancer is leading cancer in women. One in every eight to nine women has breast cancer at some point during their lifetime. Computer-Aided Diagnosis (CAD) Technology is getting more important to assist radiologists not only to detect breast cancer tumor but also to interpret lesioned regions. The CAD, as a second reader in the clinic, improves the classification of malignant and benign lesions. On the other hand, Magnetic Resonance Imaging (MRI) is a highly recommended test for detecting and monitoring breast cancer tumors and interpreting lesioned regions since it has an excellent capability for soft tissue imaging. In MRI image analysis, the segmentation images are important objective because accurate measurement of the delineation of the regions of interest (ROI) is critical for the breast cancer diagnosis and treatment. Herein, by using MRI scans, we propose a semi-automated CAD system prototype to assist radiologists in detecting breast cancer tumors and interpreting lesioned regions. The prototype, first, pre-processes the raw selected suspicious region to reduce the noises and to reveal the structure. Later, using Expectation Maximization (EM), the prototype segments the pre-processed region. After that, we use the Discrete Wavelet Transform (DWT) for providing efficient multi-resolution sub and decomposition of signals. Then Random Forest Algorithm is used for feature selection. Finally, Naive Bayes, Linear Discriminant Analysis and C4.5 Decision Tree Algorithms are used to classify the features of the ROI in the diagnosis analysis. We tested the prototype CAD on 105 patients, among them, 53 are benign and 52 malign. 80% of the images are allocated for training and 20% of images reserved for testing. The CAD classified 20 patients correctly in case of 5 fold cross-validation. Only one patient is misclassified. The computer-aided diagnosis system with the C4.5 has accuracy 95.24%. Furthermore, C4.5 classifies the breast cancer tumors better than Naive Bayes and Linear Discriminant Analysis. We tested the prototype CAD on 105 patients, among them, 53 are benign and 52 malign. The computer-aided diagnosis system with the C4.5 has accuracy 95.24%. Furthermore, C4.5 classifies the breast cancer tumors better than Naive Bayes and Linear Discriminant Analysis.*

KEY WORDS
Breast cancer, computer aided

INTRODUCTION

Breast cancer is the most common cancer among women, comprising 23% of all female cancers all over the world [1]. In Western countries, one in every eight to nine women has breast cancer at some point during their lifetime [2].

Early detection of a breast cancer tumor is crucial in the treatment process. Mammography is a valuable tool because it can identify breast cancer at an early stage, before physical symptoms develop, as a footnote, screening mammography is the only test to date proven to reduce deaths due to breast cancer [3, 4, 5, 6]. To reduce false-negative diagnosis in mammography, a biopsy is recommended for lesions with greater than a 2% chance of having suspected malignant tumors [7] and, among them, less than 30 percent are found to have malignancy [8, 9]. To reduce unnecessary biopsies, recently, Magnetic Resonance Imaging (MRI) has also been used for the diagnosis of breast cancer [10, 11] since it has an excellent capability for soft tissue imaging and the most sensitive technique in detecting breast diseases, besides, it does not contain potentially dangerous radiation [12]. But interpreting MRI images is both time-consuming and requires reader experience. In recent years, automated systems developed with computer-assisted programs have been improved to noninvasively detect abnormal lesions and determine tissue characterization in medical images. In this context, the extraction of additional features from various imaging modalities by tissue analysis has been investigated intensively. In addition, with the increasing use of medical imaging for diagnosis, treatment planning and clinical experiments, it has become almost imperative to use computers to assist radiologists in clinical diagnosis and treatment planning. Thus, Computer Aided Diagnosis (CAD) is becoming a compulsory tool in assisting radiologists not only in detecting breast cancer tumors but also in interpreting lessoned regions [13, 14]. The CAD, as a second reader in the clinic, improves classification of malignant and benign lesions [15], so it needs to be explored further. The CAD is composed of two main stages: (1) the analysis stage (2) the diagnosis stage. In the analysis stage, after the images are preprocessed, the anatomical structures of the images and their features are extracted. So, reliable methods are required for both the delineation of the regions of interest (ROI) and obtaining their features. The analysis stage consists of series of procedures such that pre-processing, segmentation and feature extraction. In the diagnosis stage, diagnosis rules are determined according to the features obtained in the analysis stage. This stage consists of classification procedure. As a result, in the CAD, there are four crucial modules: preprocessing, segmentation, feature extraction and selection, and classification.

In the literature, nevertheless, when compared to mammography and ultrasound, relatively few CAD systems have been developed for breast MRIs [16, 17]. If the CAD systems in the literature are examined,

Received: 22 June 2018
Accepted: 11 Nov 2018
Published: 20 Nov 2018

***Corresponding Author**
Email:
ahmet.yurttakal@bozok.edu.tr
Tel.: +90-354-2175064
Fax: +90-354-2171780

IIOAB JOURNAL
ISSN: 0976-3104

one can observe that K nearest neighbors (KNN) and support vector machines (SVM) are mostly used as classifiers. In addition to these, Yassin et al. in their extensive literature review study on breast cancer [18] state that there are 2 studies using Linear Discriminant Analysis (LDA) and a study using Naive Bayes, while there are no studies using decision trees as Classification Algorithm with MRI images. We detail existing researches and compare with our study in the Discussion section.

On the other hand, the segmentation module should include either breast segmentation or mass segmentation or both. Vast number of studies on mass segmentation exist in the literature, but studies on breast segmentation are limited. For more on improvements on CADs for breast cancer, see [15].

In this study, we present an alternative set of computational tools to segment and detect breast cancer tumor using MRI images. We employed the Expectation Maximization (EM) [19] to segment the ROI. Then, total of nine features are extracted, five of which are first order intensity-based statistical features [20] and four are GLCM based texture features introduced by Haralick et al. [21] in 1973. Later Random Forest Algorithm is used for feature selection and three different classification procedures (i.e. Naive Bayes, LDA, C4.5 Decision Tree Algorithm) are used. Numerical results obtained show that C4.5 Decision Tree Algorithm classifies the ROIs better than Naive Bayes, LDA.

The rest of the paper organized as follows. Sect. 2 presents the necessary materials and methods throughout the paper such that image acquisition, pre-processing, segmentation, pre-processing segmented image, feature extraction, feature selection and classification. In Sect. 3 we present some simulation results. Section 4 compares our study with the literature and presents conclusion

MATERIALS AND METHODS

The proposed CAD System is divided into five phases (i) image acquisition, (ii) ROI and segmentation of tumor region, (iii) image preprocessing, (iv) feature extraction and feature selection, (v) classification and evaluation. We tested the Proposed CAD on the dataset containing 105 patients MRI images with a dimension of 512x512 and all images are in DICOM format. Proposed CAD is implemented in the Python environment.

Image acquisition

The dataset is composed of breast MR images of patients. Breast MRI was performed at 1.5 Tesla (Achieva, Philips, The Netherlands) with the patients in a prone position using dedicated eight-channel breast coils. Non-fat suppressed T1 weighted scans in the axial plane (TR: 550 ms TE: 10 ms THK: 3 mm, FOV: 300 mm NSA: 2 T: 1.55 min), T2-weighted spoiled gradient echo (GRE) scans with fat-suppression were acquired in the axial plane (TR: 4000 ms TE: 125 ms FOV 300 mm NSA: 2 T: 1.40 min). Dynamic contrast-enhanced imaging was performed by means of a high-resolution T1-weighted gradient echo sequence with automated intravenous bolus application. Subtraction images were obtained for each contrast-enhanced series via subtraction of the non-enhanced series from the enhanced series. After performing of MRI, images were taken from MR device's workstation as DICOM images having slice thickness less than 2.0mm. As a result of image acquisition, a series of 512x512 unit16 images with 65536 different gray levels (0-65535) was obtained.

Dataset

The MRI images in the raw dataset were taken from Haseki Training and Research Hospital in. Istanbul, Turkey. The dataset consists of breast MRI images of 105 patients among them, 53 are benign and 52 malignant. Breast biopsy was performed in diagnosing tumorous regions. [Table 1] presents the characteristic of the dataset.

Table 1: Dataset characteristics

Cases	105
Benign	53
Malign	52
Image Resolution	512x512
Image Format	Dicom
Sequence	STIR
Slice Thickness	<3.00mm

Later, the dataset was randomly split into a training set and a test set. [Table 2] shows the splitting.

Table 2: Testing and training

Cases	Testing	Training
Benign	40	13
Malign	44	8

IIOAB JOURNAL
ISSN: 0976-3104

Pre-processing

Using the median filter, the noise at the intersection of the MRI image is reduced. After that, the filtered image is smoothed by Gauss filter. Then, the structural characters of the filtered image are revealed using top hat and bottom hat methods. Recall that the top hat transformation corresponds to the difference between the image and the state in which the opening operation is performed, and mathematically, defined as

$$\text{top}-\text{hat}(f,b)=f-(f\circ b) \qquad (1)$$

where $(f\circ b)$ is an opening process according to the structure b of the image f. top hat sharpens the peak values (bright areas in the image) in the image. On the other hand, bottom-hat is defined as the residual of a closing compared to the original image, mathematically,

$$\text{bottom}-\text{hat}(f,b)=(f\bullet b)-f \qquad (2)$$

Thanks to the transformation, the lower gray levels, that is, dark areas are detected. The pit areas become clear. Due to these features, top hat and bottom hat transformations help to separate the anomalies from other areas on the image [22].

Briefly, to improve contrast in the preprocessed morphotype process, the filtered image is added to the top hat filtered image and then subtracted from the bottom hat filtered image.

Segmentation of tumor using expectation maximization algorithm

Image segmentation is one of the essential steps in multi-dimensional signal processing. The purpose of the segmentation process is to cluster the intersection of the MR image pixels into salient image regions. Here, we use the Expectation Maximization (EM) method for segmenting the ROI in order to account for the spatial dependencies among pixels.

The EM algorithm [19] is an efficient iterative procedure to compute the maximum likelihood estimate in the presence of missing or unobserved latent data. The EM is perhaps most often used algorithm for unsupervised clustering.

Each iteration of the EM algorithm consists of two processes: the expectation (E-step) and the maximum likelihood (M-step). In the E-step, the missing data are estimated given the observed data and the current estimate of the model parameters. This is achieved using the conditional expectation, explaining the choice of terminology. In the M-step, the likelihood function is maximized under the assumption that the missing data are known. The estimate of the missing data from the E-step is used instead of the actual missing data. Convergence is assured since the algorithm is guaranteed to increase the likelihood at each iteration.

Processing the segmented tumor image based on 2D discrete wavelet transform

The input image represents the sum of the useful image and the noise image. Because these two random signals are not correlated, the correlation of the wavelet coefficients of the input image is the sum of the correlations of the wavelet coefficients of the useful image and of the noise image. Thus, wavelets let us analyze multi-resolution of images in detail, namely, it allows the signal to be described from the coarse level to the finest level [23, 24]. It is also useful for removing noise.

Wavelet transform plays an important role in image processing because wavelets allow both time and frequency analysis. The continuous wavelet transform of the signal $f(x)$ is defined as

$$W_{\psi}(s,\tau)=\int_{-\infty}^{\infty} f(x)\psi_{s,\tau}(x)dx \qquad (3)$$

with

$$\psi_{s,\tau}(x)=\frac{1}{\sqrt{s}}\psi\left(\frac{x-\tau}{s}\right) \qquad (4)$$

where ψ is mother wavelet, s is scaling, τ is translation. Note that Equation 3 transforms a continuous function of one variable into a continuous function of two variables.

On the other hand, in digital signal processing, a signal is represented by a discrete sequence. Thus, the discrete wavelet transform can be utilized to process it. Namely, a discrete signal $f(n), n=0,1,2,\cdots,m$ can be represented as a weighted sum of wavelets $\psi(n)$ and coarse approximation $\vartheta(n)$, mathematically,

$$f(n)=\frac{1}{\sqrt{m}}\sum_{k}W_{\vartheta}(j_0,k)\vartheta_{j_0,k}(n)+\frac{1}{\sqrt{m}}\sum_{j=j_0}^{\infty}\sum_{k}w_{\psi}(j,k)\psi_{j,k}(n) \qquad (5)$$

IIOAB JOURNAL
ISSN: 0976-3104

where j_0 is an arbitrary starting scale. In Equation 5

$$W_\psi(j,k) = \frac{1}{\sqrt{m}} \sum_{n=0}^{m} f(n) \psi_{j,k}(n) \quad (6)$$

with

$$\psi_{j,k}(n) = 2^{j/2} \psi(2^j n - k) \quad \text{and} \quad W_\vartheta(j_0,k) = \frac{1}{\sqrt{m}} \sum_{n=0}^{m} f(n) \vartheta_{j_0,k}(n) \quad (7)$$

See [23] for more details and applications of wavelet transform.

Feature extraction

Feature selection is the final processing step where feature descriptors are used to quantify characteristics of the ROI. Here we use two sets of feature families: intensity-based statistical and texture matrix-based features.

Intensity-based statistical features: The intensity-based statistical features describe how grey levels within the ROI are distributed. [Table 3] presents some intensity-based statistical features mentioned in [20]. At the table, X represents the set of N_p voxels included in the ROI and $P_{(i)}$, the first order histogram with N_g discrete intensity levels. Moreover, $p_{(i)}$ represents the normalized first order histogram. The average grey level intensity within the ROI is represented by $\bar{X}$.

Table 3: Intensity based statistical features

Statistics	Formula
Entropy	$-\sum_{i=1}^{N_g} p_{(i)} \log_2(p_{(i)} + \zeta), \zeta \approx 2.2x10^{-16}$
Mean Deviation	$\frac{1}{N_p} \sum_{i=1}^{N_p} \lvert X_{(i)} - \bar{X} \rvert$
Standard Deviation	$\sqrt{\frac{1}{N_p} \sum_{i=1}^{N_p} (X_{(i)} - \bar{X})^2}$
Skewness	$\frac{\frac{1}{N_p} \sum_{i=1}^{N_p} (X_{(i)} - \bar{X})^3}{(\sqrt{\frac{1}{N_p} \sum_{i=1}^{N_p} (X_{(i)} - \bar{X})^2})^3}$
Kurtosis	$\frac{\frac{1}{N_p} \sum_{i=1}^{N_p} (X_{(i)} - \bar{X})^4}{(\frac{1}{N_p} \sum_{i=1}^{N_p} (X_{(i)} - \bar{X})^2)^2}$

Gray level co-occurrence matrix (GLCM) based features: A statistical approach of examining texture that considers the spatial relationship of pixels (i.e. regular repetition of an element, pattern on an image) is the gray-level co-occurrence matrix (GLCM). The GLCM functions characterize the texture of an image by calculating how often pairs of pixel with specific values and in a specified spatial relationship occur in an image, creating a GLCM, and then extracting statistical measures from this matrix. The process is known as GLCM based texture analysis and gives information on the disposition of the structures and their relations with the environment [20, 25].

For a GLCM matrix of size $N_g \times N_g$, let $P_{(i,j)}$ be the co-occurrence matrix. Also, let $p_{(i,j)}$ be the normalized co-occurrence matrix. [Table 4] shows some texture features and their explanations [20].

Table 4: Texture based statistical features

Statistics	Formula
Energy	$\sum_{i}^{N_g} \sum_{j}^{N_g} p_{(i,j)}^2$
Contrast	$\sum_{i}^{N_g} \sum_{j}^{N_g} (i-j)^2 p_{(i,j)}$
Homogeneity	$\sum_{i}^{N_g} \sum_{j}^{N_g} \frac{(i-\mu_i)(j-\mu_j) p_{(i,j)}}{\sigma_i \sigma_j}$
Correlation	$\sum_{i}^{N_g} \sum_{j}^{N_g} \frac{p_{(i,j)}}{1+\lvert i-j \rvert}$

IIOAB JOURNAL
ISSN: 0976-3104

Feature selection using the random forest algorithm

Random Forests (RFs) are an elegant method for feature ranking due to their relatively good accuracy, robustness and ease of use. RF consists of a number of decision trees. Every node in the decision trees is a condition on a single feature. Here, the Gini feature importance of the RF is employed that allows for an explicit feature elimination [26]. In other words, at each node within the decision trees of the random forest, the optimal split is sought using the Gini impurity measuring how well a potential split is separating the samples of the two classes in this particular node. With correlated features, strong features can end up with low scores and the method can be biased towards variables with many categories. For the mathematical formulation of the model and its analysis, we refer readers to see [27].

Classification algorithms

Image classification is based on the assumption that the image pixels depict one or more features and that each of these features belongs to one of the several distinct and exclusive classes.

We used the features described in [Tables 3 and 4]. Here we employed three different classification methods (Naive Bayes, linear discriminant analysis, C4.5 decision tree algorithm) to classify the ROI and compared their performance.

Bayesian classifiers are among the statistical classification techniques They can predict class membership probabilities, such as the probability that a given sample belongs to a particular class.

Bayesian classifier is based on Bayes theorem, which says, for a set of classes $\Omega=\{\omega_1,\omega_2,\cdots,\omega_m\}$,

$$P(\omega_j \mid d)=\frac{P(d \mid \omega_j)P(\omega_j)}{P(d)} \tag{8}$$

where $P(\omega_j \mid d)$ is probability of instance d being in class ω_j , called posterior probability, $P(d \mid \omega_j)$ is probability of generating instance d given class ω_j , called conditional probability}, $P(\omega_j)$ is probability of occurrence of class ω_j , and $P(d)$ is probability of instance d occurring. In fact, Equation 8 is considered as Bayes classification when there is one attribute. We consider that there are more than one attributes, say n attributes. To simply task we assume that instances are independent and identically distributed. Then, given an n dimensional attribute vector $x=(x_1,x_2,\cdots,x_n)$, the class conditional probability is computed as:

$$P(x \mid \omega_j)=P(x_1 \mid \omega_j)P(x_2 \mid \omega_j)\cdots P(x_n \mid \omega_j) \tag{9}$$

and the generalization of Equation 8 is

$$P(\omega_j \mid x)=\frac{P(x \mid \omega_j)P(\omega_j)}{P(x)} \tag{10}$$

Naive bayes classification is the most likely or maximum posterior class that solves the optimization problem:

$$\arg_{\omega\in\Omega}\max P(\omega \mid \mathrm{x}) \tag{11}$$

Note that, in solving the optimization problem, we disregard the denominator $P(x)$ in Equation 10.

Naive Bayesian classifier assumes that the features in a dataset are mutually independent. In practice, the independence assumption is often violated, but naive Bayes classifiers still tend to perform very well under this unrealistic assumption [28].

Linear Discriminant Analysis (LDA), developed in 1936 by R. A. Fisher [29], searches for a linear combination of variables that best separates two or more classes. Suppose that the class set $\Omega=\{\omega_1,\omega_2\}$ has two classes and we need to discriminate between them. Then, we classify d d dimensional sample $\phi=\{x_1,x_2,\cdots,x_d\}$, let

$$Z=\beta_1 x_1+\beta_2 x_2+\cdots+\beta_d x_d \tag{12}$$

where $\beta_1,\beta_2,\cdots,\beta_d$ are unknowns and called predictors. The main objective of LDA is to find a linear combination of variables, as in Equation 12, that gives the maximum class separability. To reach this, Fisher defined the following score function

IIOAB JOURNAL
ISSN: 0976-3104

$$S(\beta) = \frac{\beta^T \mu_1 - \beta^T \mu_2}{\beta^T C \beta} \quad (13)$$

where $\beta = (\beta_1, \beta_2, \cdots, \beta_d)$ is the linear model coefficients vector, μ_1 and μ_2 are the mean vectors of the classes ω_1 and ω_2, respectively, and C is the pooled within group covariance matrix. In this method, we need to estimate the linear coefficients that maximize the score function to maximize the score function to maximize the discrimination between two considered classes. One can compute β and C as

$$\beta = C^{-1}(\mu_1 - \mu_2) \quad (14)$$

$$C = \frac{1}{d_1 + d_2}(d_1 \operatorname{cov}(\omega_1) + d_2 \operatorname{cov}(\omega_2)) \quad (15)$$

where $\operatorname{cov}(\mu_i)$ is covariance matrix for the class i and d_i is the number of observations in the class.

C4.5 is arguably the most popular algorithm used to generate DTs. C4.5 owes its popularity to solving various problems, such as continuous attributes and missing attribute values [30]. It is more robust in the presence of noise.

C4.5 uses gain ratio, evaluated by entropy, as an attribute selection measure to build a decision tree. Let S be the set of samples with n classes. Then the entropy of S is defines as

$$E(S) = -\sum_{i=1}^{n} p_i \log p_i \quad (16)$$

where p_i is the proportion of samples in S that belong to the i th class. When an attribute A splits the set S into subsets S_i, the average entropy (a.k.a information) is defined as

$$I(S, A) = \sum_i \frac{|S_i|}{|S|} E(S_i) \quad (17)$$

and information gain for the attribute A as

$$Gain(S, A) = E(S) - I(S, A) \quad (18)$$

Moreover, intrinsic information of the split A is

$$InstI(S, A) = \sum_i \frac{|S_i|}{|S|} \log(\frac{|S_i|}{|S|}) \quad (19)$$

and gain ratio

$$GA(S, A) = \frac{Gain(S, A)}{InstI(S, A)} \quad (20)$$

At each node in the DT, the attribute with the highest information gain ratio is chosen.

RESULTS AND DISCUSSION

The CAD is implemented in the Python environment. We tested the CAD on the dataset containing 105 patients MRI images, among them, 53 are benign and 52 malign, These MRI images are obtained from local hospital in Turkey.

Data exploring

Intersection of MRI image at [Fig. 1(a)] is pre-processed to obtain [Fig. 1(b)]. During the pre-processing procedure, the original image is applied to median filter for reducing the noise, and then gaussian filter for smoothing the image. After that, top hat and bottom hat operations are performed to the resulting image. Then, ROI, ellipse region in [Fig. 1(b)], is selected. Later, the ROI is pre-processed to obtain [Fig. 2(a)] then, segmented via EM clustering technique to obtain [Fig. 2(b)]. The segmented images, then, is applied to 2D-discrete wavelet transform before texture analysis. [Fig. 3] presents the texture analysis results.

IIOAB JOURNAL
ISSN: 0976-3104

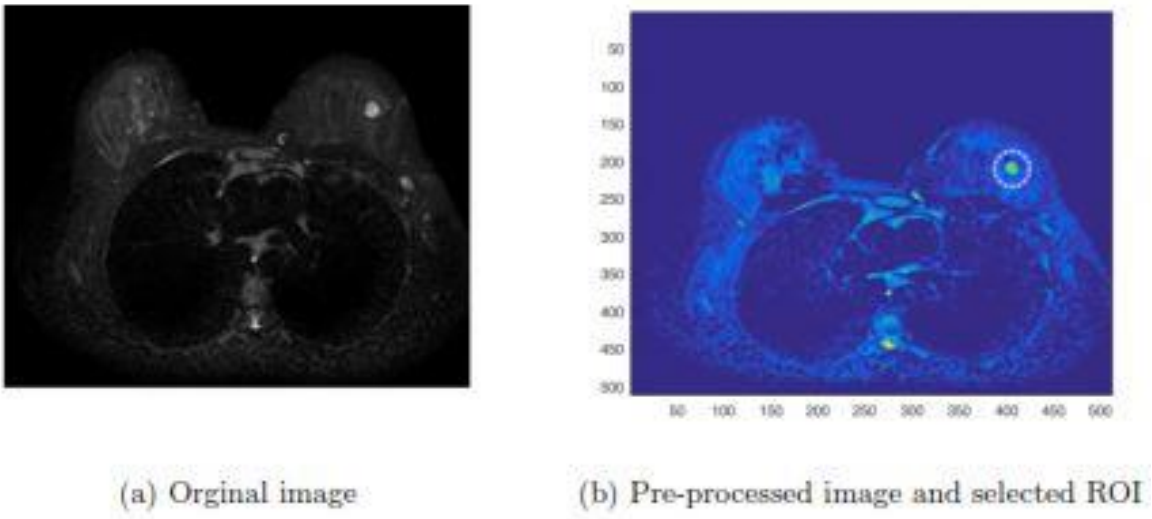

(a) Orginal image (b) Pre-processed image and selected ROI

Fig. 1: Original image (a) is processed to obtain (b) and the ROI is selected.

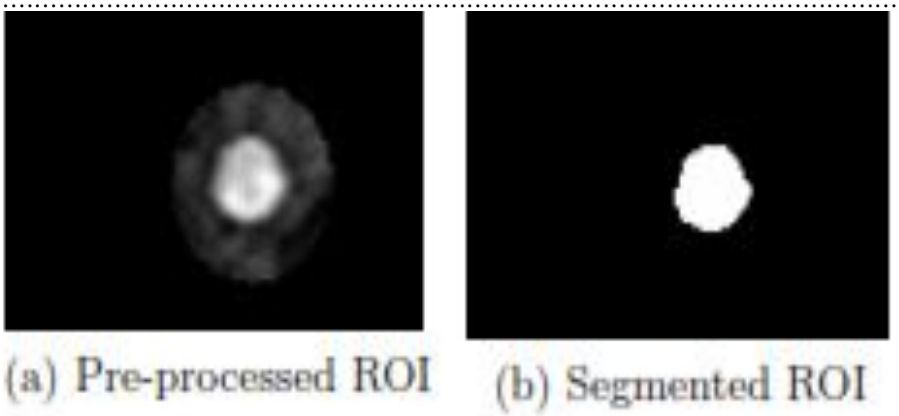

(a) Pre-processed ROI (b) Segmented ROI

Fig. 2: Pre-processed ROI (a) is segmented to obtain (b).

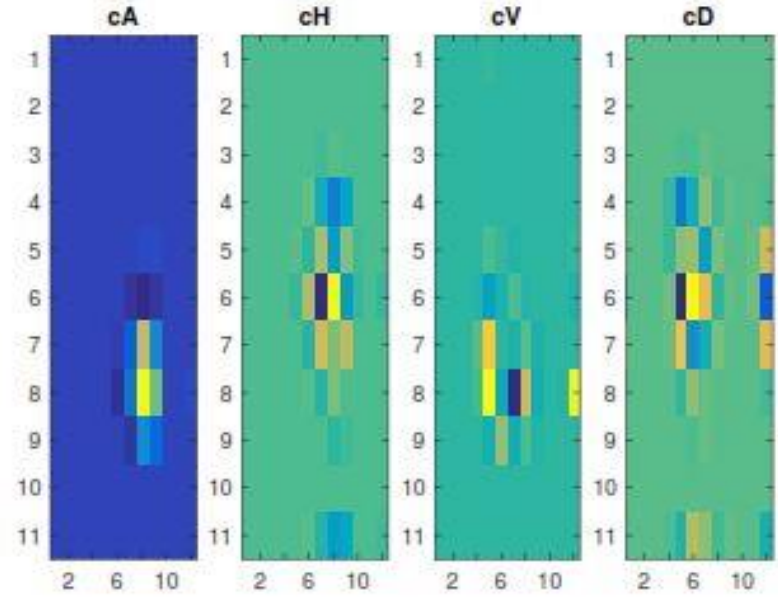

Fig. 3: Wavelet texture of segmented ROI by EM.

[Table 5] presents quantitative values of the features described in [Tables 3 and 4] in the dataset.

IIOAB JOURNAL
ISSN: 0976-3104

Table 5: Statistic of features in the dataset

	Contrast	Correlation	Energy	Homogeneity	Mean	Std_Dev	Entropy	Kurtosis	Skewness
mean	1.090130	0.111163	0.540387	0.844589	0.014990	0.156886	3.732237	6.300306	0.856687
std	0.304420	0.076212	0.086720	0.033901	0.007165	0.012822	0.341759	1.938972	0.299210
min	0.579670	-0.052528	0.342828	0.756250	-0.006134	0.132644	2.986560	3.483746	0.255409
max	1.772321	0.269580	0.683801	0.892634	0.031909	0.176936	4.237545	12.198865	1.605046

[Fig. 4] shows violin plot that is used to visualize the distribution of the data and the probability density. According to the figure, the median of contrast, homogeneity, energy and standard deviation might give good results in the classification. However, the median value of the correlation and mean properties may not give good results in classification.

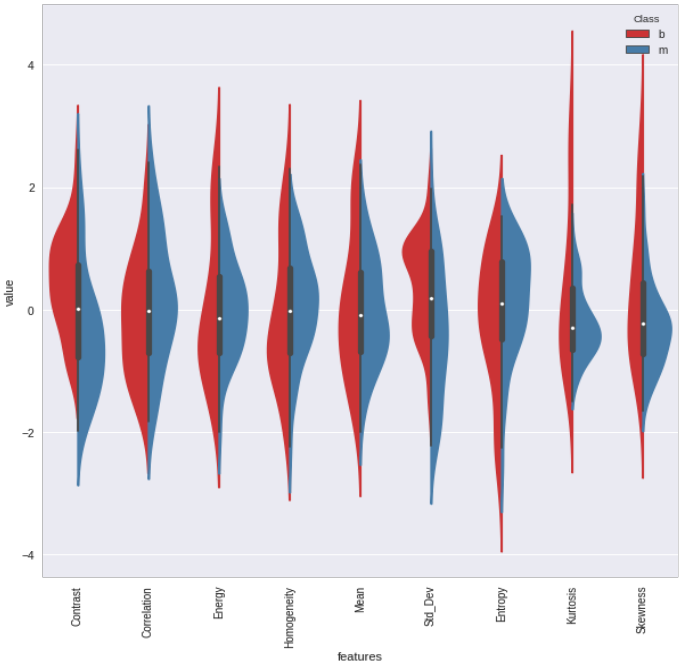

Fig. 4: Violin Plot for data visualization.

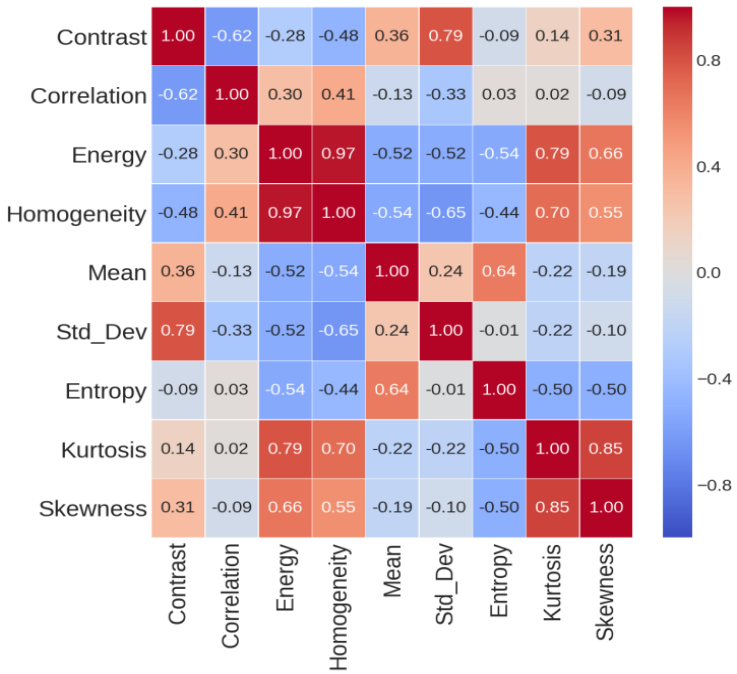

Fig. 5: Correlation matrix.

IIOAB JOURNAL
ISSN: 0976-3104

[Fig. 5] shows heat map for correlation. Correlation is a bivariate analysis that measures the strength of association between two variables and the direction of the relationship. In terms of the strength of relationship, the value of the correlation coefficient varies between +1 and -1. A value of ±1 indicates a perfect degree of association between the two variables. As the correlation coefficient value goes towards 0, the relationship between the two variables will be weaker. The direction of the relationship is indicated by the sign of the coefficient; a + sign indicates a positive relationship and a – sign indicates a negative relationship. According to the figure, Contrast, Standard Deviation, Energy, Homogeneity, Kurtosis, Skewness data are correlated. These features may be useful in classification

In random forest classification method there is a feature importance's attributes. [Fig. 6] shows feature importance's. The green bars are the feature importance's of the forest, along with their inter-trees variability. The plot shows that 4 features are more informative and the rest are less informative.

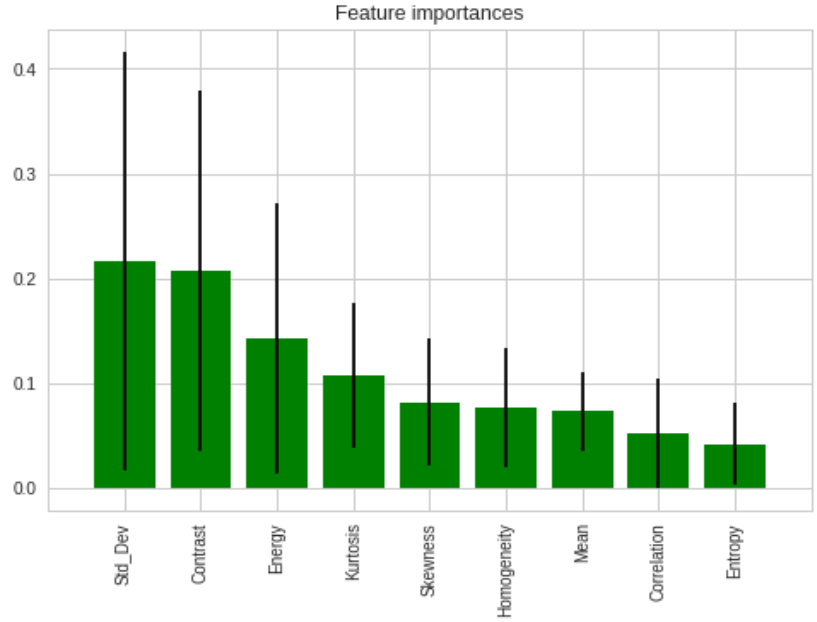

Fig. 6: Feature Importance's.

Classification Performance

A model that would just repeat the labels of the samples that it has just seen would have a perfect score but would fail to predict anything useful on yet. To avoid it, 84 patients' images are allocated for training and 21 patients' images reserved for testing. Three different classification algorithms (Naive Bayes, the LDA and C4.5) are fed separately with these features. [Fig. 7] shows confusion matrix. According to the figure, C4.5 Decision Tree Algorithm classified 20 patients correctly with a success rate of 95.24%. Only one patient is misclassified. Naive Bayes Algorithm classified 19 patients correctly with a success rate of 90.48%. LDA Algorithm classified 18 patients correctly with a success rate of 85.71%.

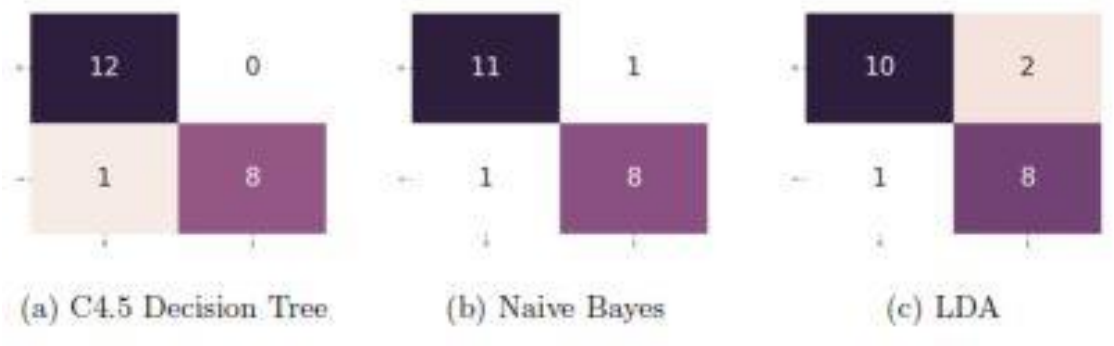

Fig. 7: Confusion Matrix.

The features selected in the random forest feature selection are used to train the C4.5 Decision Tree, Naive Bayes and LDA classifiers by 5-fold cross validation method. Using some metrics such that precision, recall and F-beta score, we compare the performance of the three algorithms. These metrics of the

IIOAB JOURNAL
ISSN: 0976-3104

classifiers are tabulated in [Table 6]. Observe that C4.5 Decision Tree Algorithm has better classification accuracy than the others.

Table 6: Classification Report

	C 4.5 Decision Tree	Naive Bayes	LDA
Precision	1.000	0.889	0.800
Recall	0.889	0.889	0.889
F1 Score	0.941	0.829	0.842
Mean Auc	0.800	0.790	0.600
Accuracy	0.9524	0.9048	0.8571

As we mentioned above, in the CAD, there are four crucial modules: preprocessing, segmentation, feature extraction and selection, and classification. The preprocessing module prepares the images for the subsequent stages and responsible for cleaning the medical image and removing noise from it through a set of image preprocessing operations. The segmentation module, in fact, is a procedure of dividing the input image into several regions according to the visual characteristics. In the features extraction and selection module, features are extracted from the cleaned images, then the most discriminative features are selected. The selected features are capable of differentiating between normal and cancerous regions in order to minimize the classification error. Despite the large effort, there is still no agreement on the features that are most suitable for the target task. Many kinds of features such as dynamic features, textural features, and morphological features have been traditionally used in tumor classification. Along with the segmentation, the classification module is regarded as the heart of the CAD.

Karaçavuş et al. [31] used otsu segmentation and the KNN classifier in the TNM staging system they developed and achieved a result of 84% accuracy. In their study, they extracted ten textual features and among them they used five features in classification of tumor stage. Waugh et al. [32] achieved 74.7% accuracy using KNN classification. On the other side, Cai et al. [33] analyzed the effects of 28 features in four different classes to the dataset collected under different imaging protocols, in result, they obtained that instead of using all features only five features with the highest diagnostic affect rates have the highest classification accuracy of 82.8% using SVM. They incorporated fuzzy c-means clustering and a gradient vector flow snake algorithm to segment the ROI.

The first time in the literature in breast MRI, we used the EM method to segment ROI which is the crutial step in the CAD. Later, carefully selected total nine features, among them five from intensity-based statistical and four from texture matrix-based features, fed to a classifier, in particular, C4.5 decision tree classification.

CONCLUSION

In this paper, we presented a novel user-independent time-saving CAD to diagnose breast cancer tumor using MRI images. The CAD is composed of two main stages: (1) the analysis stage (2) the diagnosis stage. On the other side, the analysis stage consists of series of procedures such that pre-processing, segmentation and feature extraction. The CAD uses the EM for segmenting the ROI. Later, some intensity-based statistical and texture matrix-based features are obtained. Finally, using three different methods such that C4.5 Decision Tree, Naive Bayes and LDA, the ROI is classified.

Experimental results indicate that the EM segmentation and C4.5 classifications, having accuracy 95.24%, successfully distinguish the tumor's region from the other regions.

CONFLICT OF INTEREST
There is no conflict of interest.

ACKNOWLEDGEMENTS
None

FINANCIAL DISCLOSURE
None

REFERENCES

[1] Ozmen V. [2008] Breast cancer in the world and Turkey. J Breast Health. 4(2):6-12.
[2] Aydıntuğ S. [2004] Meme kanserinde erken tanı. Sted. 13(6):226-229.
[3] Cady B, Michaelson JS. [2001] The life-sparing potential of mammographic screening. Cancer: Interdisciplinary International Journal of the American Cancer Society. 91(9):1699-1703.
[4] Smith RA, Cokkinides V, von Eschenbach AC, et al. [2002] American Cancer Society guidelines for the early detection of cancer. CA: a cancer journal for clinicians. 52(1):8-22.
[5] Feig SA, D'Orsi CJ, Hendrick RE, et al. [1998] American College of Radiology guidelines for breast cancer screening. AJR. American journal of roentgenology. 171(1):29-33.
[6] Berg WA. [2010] Benefits of screening mammography. Jama. 303(2):168-169.
[7] Sickles EA. [1991] Screening for breast cancer with mammography. Clinical imaging. 15(4):253-260.

IIOAB JOURNAL
ISSN: 0976-3104

[8] Adler DD, Helvie, MA. [1992] Mammographic biopsy recommendations. Current Opinion in Radiology. 4(5):123-129.
[9] Sickles EA. [1991] Periodic mammographic follow-up of probably benign lesions: results in 3,184 consecutive cases. Radiology. 179(2):463-468.
[10] Prince JL, Links JM. [2006] Medical imaging signals and systems. Upper Saddle River, NJ: Pearson Prentice Hall.
[11] Wollins DS, Somerfield MR. [2008] Q and a: magnetic resonance imaging in the detection and evaluation of breast cancer. Journal of oncology practice. 4(1):18-23.
[12] Kuhl C. [2007] The current status of breast MR imaging part I. Choice of technique, image interpretation, diagnostic accuracy, and transfer to clinical practice. Radiology. 244(2):356-378.
[13] Deurloo EE, Muller SH, Peterse JL, Besnard AP, Gilhuijs KG. [2005] Clinically and mammo graphically occult breast lesions on MR images: potential effect of computerized assessment on clinical reading. Radiology. 234(3):693-701.
[14] Nattkemper TW, Arnrich B, Lichte O, et al. [2005] Evaluation of radiological features for breast tumour classification in clinical screening with machine learning methods. Artificial intelligence in medicine. 34(2):129-139.
[15] Hadjiiski L, Sahiner B, Chan HP. [2006] Advances in CAD for diagnosis of breast cancer. Current opinion in obstetrics & gynecology. 18(1):64.
[16] Levman JE, Warner E, Causer P, Martel AL. [2014] A vector machine formulation with application to the computer-aided diagnosis of breast cancer from DCE-MRI screening examinations. Journal of digital imaging. 27(1):145-151.
[17] Shi J, Sahiner B, Chan HP, et al. [2009] Treatment response assessment of breast masses on dynamic contrast-enhanced magnetic resonance scans using fuzzy c-means clustering and level set segmentation. Medical physics. 36(11):5052-5063.
[18] Yassin NI, Omran S, El Houby EM, Allam H. [2017] Machine learning techniques for breast cancer computer aided diagnosis using different image modalities: a systematic review. Computer methods and programs in biomedicine.
[19] Dempster AP, Laird NM, Rubin DB. [1977] Maximum likelihood from incomplete data via the EM algorithm. Journal of the royal statistical society. Series B (methodological). 1-38.
[20] Zwanenburg A, Leger S, Vallières M, Löck S. [2016] Image biomarker standardization initiative. arXiv preprint arXiv:1612.07003.
[21] Haralick RM, Shanmugam K. [1973] Textural features for image classification. IEEE Transactions on systems, man, and cybernetics. (6):610-621.
[22] Burçin KURT, NABİYEV VV. [2010] Dijital mamografi görüntülerinin kontrast sınırlı adapt if histogram eşitleme ile iyileştirilmesi.
[23] Debnath L, Shah FA. [2002] Wavelet transforms and their applications. Boston: Birkhäuser. 2-14.
[24] Stollnitz EJ, DeRose AD, Salesin DH. [1995] Wavelets for computer graphics: a primer. 1. IEEE Computer Graphics and Applications. 15(3):76-84.
[25] Pathak B, Barooah D. [2013] Texture analysis based on the gray-level co-occurrence matrix considering possible orientations. International Journal of Advanced Research in Electrical, Electronics and Instrumentation Engineering. 2(9):4206-4212.
[26] Menze BH, Kelm BM, Masuch R, et al. [2009] A comparison of random forest and its Gini importance with standard chemometric methods for the feature selection and classification of spectral data. BMC bioinformatics. 10(1):213.
[27] Biau G. [2012] Analysis of a random forests model. Journal of Machine Learning Research. 13:1063-1095.
[28] Rish I. [2001] An empirical study of the naive Bayes classifier. In IJCAI 2001 workshop on empirical methods in artificial intelligence. New York: IBM. 3(22):41-46.
[29] Fisher RA. [1936] The use of multiple measurements in taxonomic problems. Annals of eugenics. 7(2):179-188.
[30] Quinlan JR. [2014] C4. 5: programs for machine learning. Elsevier.
[31] Karacavus S, Yılmaz B, Tasdemir A, et al. [2018] Can Laws Be a Potential PET Image Texture Analysis Approach for Evaluation of Tumor Heterogeneity and Histopathological Characteristics in NSCLC? Journal of digital imaging. 31(2):210-223.
[32] Waugh SA, Purdie CA, Jordan LB, et al. [2016] Magnetic resonance imaging texture analysis classification of primary breast cancer. European radiology. 26(2):322-330.
[33] Cai H, Liu L, Peng Y, Wu Y, Li L. [2014] Diagnostic assessment by dynamic contrast-enhanced and diffusion-weighted magnetic resonance in differentiation of breast lesions. BMC Cancer.14:366.